


Current and emerging approaches to noncompetitive AR inhibition

Christopher M. Riley¹ | Jessica M. L. Elwood¹ |
Martyn C. Henry¹  | Irene Hunter² |
J. Daniel Lopez-Fernandez¹ | Iain J. McEwan² | Craig Jamieson¹

¹Department of Pure and Applied Chemistry, University of Strathclyde, Glasgow, UK

²Institute of Medical Sciences, University of Aberdeen, Aberdeen, UK

Correspondence

Craig Jamieson, Department of Pure and Applied Chemistry, University of Strathclyde, 295 Cathedral St, Glasgow G1 1XL, UK.
Email: craig.jamieson@strath.ac.uk

Iain J. McEwan, Institute of Medical Sciences, University of Aberdeen, Foresterhill, Aberdeen AB25 2ZD, UK.
Email: iain.mcewan@abdn.ac.uk

Abstract

The androgen receptor (AR) has been shown to be a key determinant in the pathogenesis of castration-resistant prostate cancer (CRPC). The current standard of care therapies targets the ligand-binding domain of the receptor and can afford improvements to life expectancy often only in the order of months before resistance occurs. Emerging preclinical and clinical compounds that inhibit receptor activity via differentiated mechanisms of action which are orthogonal to current antiandrogens show promise for overcoming treatment resistance. In this review, we present an authoritative summary of molecules that noncompetitively target the AR. Emerging small molecule strategies for targeting alternative domains of the AR represent a promising area of research that shows significant potential for future therapies. The overall quality of lead candidates in the area of noncompetitive AR inhibition is discussed, and it identifies the key chemotypes and associated properties which are likely to be, or are currently, positioned to be first in human applications.

KEYWORDS

androgen receptor, developability properties, noncompetitive inhibition, prostate cancer

This is an open access article under the terms of the Creative Commons Attribution License, which permits use, distribution and reproduction in any medium, provided the original work is properly cited.

© 2023 The Authors. *Medicinal Research Reviews* published by Wiley Periodicals LLC.

1 | INTRODUCTION

Despite decades of research, prostate cancer remains the second most common cancer in men with estimates exceeding 1.4 million new diagnoses and 370,000 deaths worldwide in 2020.¹ With the advent of modern screening techniques enabling earlier detection and intervention, primary localized therapy can successfully treat 65%–80% of prostate cancer cases. However, for the proportion of patients that relapse, disease progression to castration-resistant prostate cancer (CRPC) invariably occurs.^{2–4} Upon relapse, systemic treatment is pursued in the form of androgen deprivation therapy (ADT), which is achieved by surgical and/or chemical castration and reduces serum androgen levels by up to 95%.⁵ These approaches have been developed over the last several decades since the pioneering discoveries by Charles Huggins in 1941, where he described how surgical and chemical castration reduces androgen levels, leading to tumor regression and symptom alleviation.⁶ Although ADT affords an initial improvement, progression to CRPC usually occurs within 12–48 months, at which point, further treatment is limited to radiotherapy or chemotherapy, with the median survival ranging from 9 to 30 months.^{7,8} Recent efforts to develop new treatments have been relatively successful. Indeed, with the introduction of new antiandrogenic drugs such as enzalutamide (nonsteroidal) and abiraterone (steroidal), the patient outlook has improved, with a 15% increase in 5-year overall survival.⁹ Nevertheless, the prognosis for CRPC remains poor and the need for continued improvement of its treatment is clear.

At the core of the pathogenesis of prostate cancer is the androgen receptor (AR), a 110 kDa nuclear receptor (NR) primarily responsible for the androgen-mediated regulation of gene expression. Its function is vital for the growth and maintenance of both normal and carcinogenic prostate tissue.¹⁰ The AR protein consists of four domains: the C-terminal ligand-binding domain (LBD) where the ligand-binding pocket (LBP) resides, the DNA-binding domain (DBD), the amino-terminal domain (NTD), and a hinge region that connects the LBD and the DBD (Figure 1).

The AR gene is commonly mutated in prostate cancer and the receptor itself has been extensively validated as a drug target.¹¹ When disease progression to CRPC occurs, the AR remains a potent driver for cancer growth and metastasis.^{12,13} There is considerable evidence implicating the aberrant activation of the AR during ADT as a potential cause for the development of CRPC.^{11–13} Antiandrogens are antagonists that compete with androgens to bind the AR-LBP and have been one of the most significant targets for drug development for CRPC therapies. Steroidal and more recently nonsteroidal compounds have been developed for the treatment of advanced and metastatic prostate cancer in recent decades.^{14–16} Although these drugs are initially successful, a complex variety

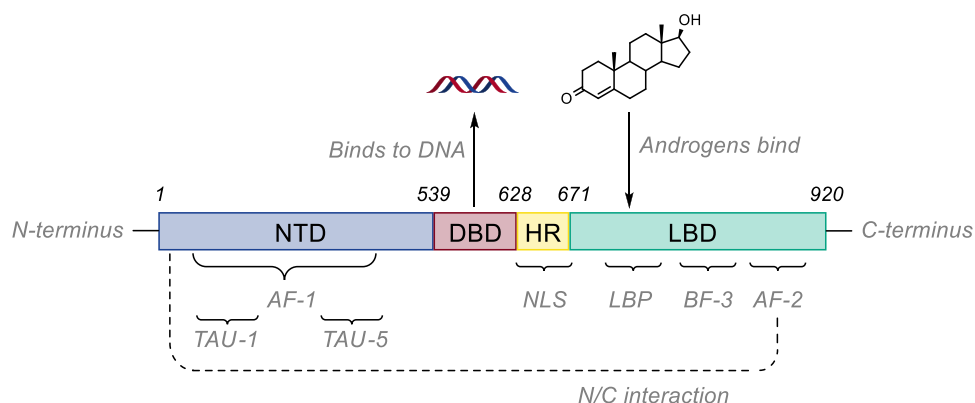


FIGURE 1 Structure of the androgen receptor. AF, activation function; BF, binding function; DBD, DNA-binding domain; HR, Hinge region; LBD, ligand-binding domain; LBP, ligand-binding pocket; NLS, nuclear localization signal; NTD, N-terminal domain; TAU, transactivation unit. [Color figure can be viewed at [wileyonlinelibrary.com](https://onlinelibrary.wiley.com/doi/10.1002/mr.2001)]

of resistance mechanisms have emerged that drive tumor progression. The development of treatment resistance and potential methods of overcoming it has garnered significant interest in recent years.^{12,17–19} Emerging approaches have shifted attention away from the LBP, focussing on the development of compounds that target the AR protein via alternative domains.^{20–22}

In the current review, our aim is to provide a detailed account of contemporary treatments that target the AR beyond the LBP and to critically evaluate the developability of emerging lead compounds. The direct comparison of compounds reported herein is intrinsically difficult due to the heterogeneous nature of the reported data, which spans multiple laboratories, and the variety of biological assays utilized. Hence, a compound-by-compound approach will be taken, outlining activity against full-length AR (AR-FL) and mutant variants, lacking the LBD (AR-V) commonly associated with CRPC, such as AR-V7.²³ Our analysis aims to highlight structural properties from a medicinal chemistry perspective and employs the use of *in silico* physicochemical property prediction data. Due to the multifaceted nature of lead optimization impacting on the potency, selectivity, drug metabolism, and pharmacokinetics (DMPK) of a specific compound, attention will be paid to several developability metrics and molecular properties that can be used to characterize candidate drugs. Of particular importance throughout this review are molecular weight (MW), topological polar surface area (TPSA), calculated lipophilicity coefficient (cLogP) calculated using the open source software DataWarrior, number of hydrogen bond donors (HBD) and hydrogen bond acceptors (HBA) defined by Lipinski's rules,^{24,25} and intrinsic property forecast index (iPFI), a metric proposed by Young et al. that is the sum of cLogP and aromatic ring count which is correlated with important considerations such as solubility and off-target effects.²⁶

2 | TARGETING THE LBD

Currently, there are several approved nonsteroidal antiandrogen drugs such as *flutamide*, *bicalutamide*, and *enzalutamide* which share a structural motif—an anilide-bearing electron-withdrawing cyano, nitro, and/or trifluoromethyl groups. Contemporary antiandrogens *apalutamide* and *darolutamide* deviate slightly from this, incorporating a pyridine ring and omitting the anilide moiety, respectively; however, they maintain a degree of structural similarity with their predecessors (Figure 2).

Several molecular properties can give discovery teams an indication of how a given molecule might behave *in vivo*, particularly pertaining to MW and LogP. These properties allow insight into the dynamics of ADME behavior; that is, how a molecule is absorbed, distributed, metabolized, and excreted from a site of action.²⁷ The compounds shown in Figure 2 will be nonionized under physiological conditions, and despite their low aqueous solubility, are well absorbed in the gastrointestinal tract, likely due to good permeability as demonstrated experimentally using Caco-2 cells.²⁸ Oral absorption of these drugs is good, except for *darolutamide* which is considered to be moderate.²⁹ The high bioavailability observed in the remaining examples can be attributed to cLogP values in the range of 2.0–3.6, MWs below 500 Da, and a minimal rotatable bond count.³⁰ *Enzalutamide* can penetrate the blood–brain barrier (BBB), possibly due to a low TPSA (<110 Å), giving rise to off-target effects at the γ -aminobutyric acid receptor, presenting a potential risk of seizure.¹⁵ Next-generation analogs, *apalutamide* and *darolutamide* mitigated these risks via reduced penetration of the BBB and have also displayed efficacy in enzalutamide-resistant models of CRPC.^{15,31} Despite these advancements resistance eventually occurs, warranting further investigation of novel treatments.³²

The current understanding of AR-dependant resistance mechanisms include the following: (1) constitutively or conditionally active AR-Vs which lack the LBD entirely, (2) AR point mutations that can confer ligand promiscuity or increased stability to degradation, (3) gene amplification and receptor overexpression, (4) intra-tumoural or adrenal androgen synthesis, (5) interference with AR coregulation, and (6) ligand-independent receptor activation.^{17,19,33–35} Some of these mechanisms do not rely on the availability of androgens or antiandrogens; thus, the exclusive

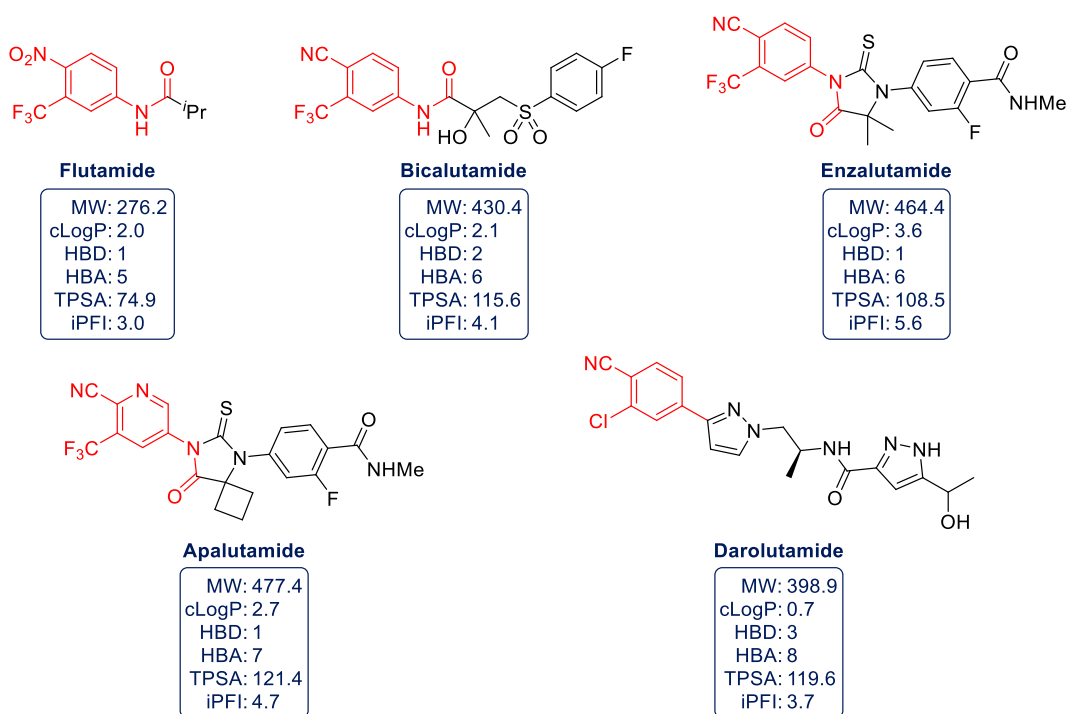


FIGURE 2 Prevailing clinical antiandrogens with highlighted shared/similar motif. cLogP, calculated lipophilicity coefficient; HBA, hydrogen bond acceptor; HBD, hydrogen bond donors; iPFI, intrinsic property forecast index; MW, molecular weight; TPSA, topological polar surface area. [Color figure can be viewed at wileyonlinelibrary.com]

development of LBP antagonists is likely to encounter resistance similar to current treatments. This can be observed in reports of receptor point mutations and splice variants giving rise to enzalutamide resistance.^{36,37}

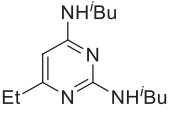
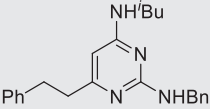
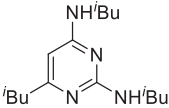
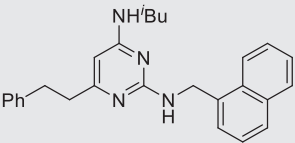
3 | ACTIVATION FUNCTION 2-TARGETING COMPOUNDS

When agonists bind to the LBP, a conformational change occurs, forming activation function 2 (AF-2)—a surface-accessible hydrophobic pocket available for protein–protein interactions (PPIs).^{38–40} The AF-2 region interacts with cofactors, the NTD, and the LBD, making it an attractive target to regulate AR activity via orthosteric inhibition of key PPIs.^{41,42} The AF-2 domain has been validated as a route for inhibition using peptide antagonists with multiple supporting studies.^{43–45} Based on this, the following small molecules have been identified or designed to directly, orthosterically disrupt the interaction between the AR AF-2 and coregulatory proteins in the AR signaling pathway.

The development of small molecule coactivator binding inhibitors was described by Gunther et al. in 2009.⁴⁶ A pyrimidine-core estrogen receptor (ER) AF-2 inhibitor was modified, increasing the steric bulk of side chains, thus affording selectivity for the AR AF-2 over other hormone receptors, exemplified by Compound 7 (Table 1). The series displayed efficacy against both wild-type AR (AR-WT) and the flutamide-resistant T877A mutant with IC₅₀ values of 1.6 and 9.4 μ M, respectively, in a luciferase assay. Noncompetitive receptor inhibition with respect to dihydrotestosterone (DHT), as well as a radiometric binding assay using tritium-labeled synthetic androgen R1881, both provide evidence for orthosteric inhibition of the AR-steroid receptor coactivator (AR-SRC) interaction.

Initially developed as structure-based peptidomimetics, the introduction of flexible aliphatic chains (compound 1 and 3) and several aromatic rings (compound 2 and 7) afforded specificity toward the desired target. However,

TABLE 1 Peptidomimetic ER/AR AF-2 inhibitors.

Compound	Structure	Properties	IC ₅₀ (μM) ⁴⁶		
			ER	AR-WT	AR-T877A
1		MW: 250.4 cLogP: 3.1 HBD: 2 HBA: 4 TPSA: 49.8 iPFI: 4.1	7.9	No binding	7.4
2		MW: 360.5 cLogP: 4.9 HBD: 2 HBA: 4 TPSA: 49.8 iPFI: 7.9	4.1	2.6	3.5
3		MW: 278.4 cLogP: 3.8 HBD: 2 HBA: 4 TPSA: 49.8 iPFI: 4.8	3.6	5.6	7.1
7		MW: 410.6 cLogP: 6.1 HBD: 2 HBA: 4 TPSA: 49.8 iPFI: 10.1	>30	1.6	9.4

Note: All values obtained by luciferase reporter gene assay.

Abbreviations: AF-2, activation function 2; AR-WT, wild-type androgen receptor; cLogP, calculated lipophilicity coefficient; ER, estrogen receptor; HBA, hydrogen bond acceptor; HBD, hydrogen bond donors; iPFI, intrinsic property forecast index; MW, molecular weight; TPSA, topological polar surface area.

these structural features also contribute to increased lipophilicity, which could lead to off-target effects, albeit toxicity was not seen at even high concentrations.⁴⁷ The main drawback of these compounds remains poor solubility; however, this could be circumvented via the incorporation of heterocycles and polar substituents into the peripheral aromatic rings.

Computer-aided drug discovery approaches have been used to screen the ZINC lead-like database—a curated collection of approximately 4 million biologically relevant compounds.⁴⁸ Utilizing a docking study, combined with experimental approaches, Axerio-Cilies et al. identified two hits, compounds **4** and **6** that bound directly and specifically to AF-2 to inhibit recruitment of AR coactivator SRC2 (Figure 3).⁴⁹

The more potent analog, compound **4**, displaced SRC2 with an IC₅₀ of 8.2 μM and inhibited AR transactivation with an IC₅₀ of 34.4 μM determined by a nondestructive cell-based enhanced green fluorescent protein (eGFP) assay (Table 2); compound **6** performed similarly in the eGFP assay and was threefold less potent in the SRC displacement assay. Direct and reversible interaction between the compounds and the AR was established via biolayer interferometry (BLI). Any interaction with the LBP was excluded via an androgen displacement assay. Moreover, a crystal structure was determined with a closely related analog (compound **5**) shown to be directly situated at AF-2 (Figure 4).

Compounds **4** and **6** both comply with Lipinski's rules, and the cLogP and iPFI imply good solubility; however, the presence of polar groups combined with relatively low lipophilicity could potentially have a negative impact on membrane permeability. Compound **4** did not show toxicity liabilities; however, compound **6** displayed cytotoxicity in an MTS assay (50% inhibition at 50 μM) which could be ascribed to the hydrazide moiety, a known toxicophore.⁶⁰

A further virtual screening campaign for AF-2 antagonists yielded a diarylhydrazide series typified by **MDG506**, which inhibited AR-WT and T877A in a TR-FRET assay with IC₅₀ values of 26 and 33 μM, respectively (Figure 5A).⁵⁰ Lloyd et al. highlighted the potentially problematic electrophilic hydrazide linker necessitating

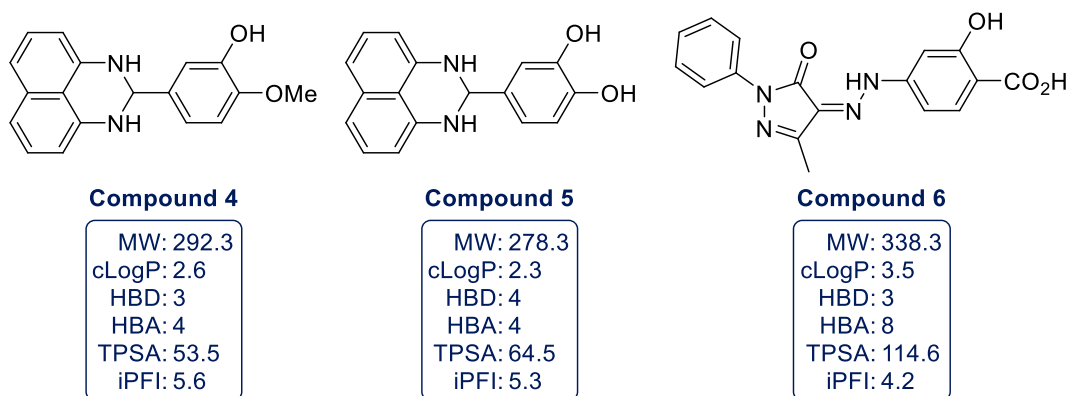


FIGURE 3 Activation function 2 inhibitors developed using computer-aided drug discovery. cLogP, calculated lipophilicity coefficient; HBA, hydrogen bond acceptor; HBD, hydrogen bond donors; iPFI, intrinsic property forecast index; MW, molecular weight; TPSA, topological polar surface area. [Color figure can be viewed at wileyonlinelibrary.com]

TABLE 2 Inhibitory activity and assay description of AF-2 targeting compounds.

Compound	Reported activity (IC ₅₀)		Assay description
	AR-WT (μM)	AR-T877A (μM)	
7 ⁴⁶	1.6	9.4	MMTV-luciferase assay in HEC-1 cells
4 ⁴⁸	34.4	–	eGFP assay in LNCaP cells
	8.2	–	Fluorescence polarization assay for SRC2-3 displacement
6 ⁴⁸	33.4	–	eGFP assay in LNCaP cells
	26	–	Fluorescence polarization assay for SRC2-3 displacement
MDG506 ⁵⁰	26.3	33.2	TR-FRET assay
SPC002 ^{51,52}	24	–	TR-FRET assay
7b ⁵³	≤40	–	MMTV-luciferase assay in CV-1 cells
D2 ⁵⁴	0.04*	–	Co-IP assay for AR-PEPL1 interaction in LNCaP cells/*confirmed by CyQuant proliferation assay
14d ⁵⁵	0.016	–	MTT cell viability assay in LNCaP cells
TPCK ⁵⁶	0.764/2.4*	–	AR-RFP TIF2-GFP biosensor assay in U-2OS/*AR-transfected PC-3 cells
Parthenolide ⁵⁶	1.17/0.925*	–	AR-RFP TIF2-GFP biosensor assay in U-2OS/* AR-transfected PC-3 cells
LHJ-647 ⁵⁷	1	–	MMTV-luciferase assay in PC-3 cells
IMB-A6 ⁵⁸	10*	–	PSA-Luciferase in LNCaP cells/*confirmed in AR-transfected PC-3 cells
T1-12 ⁵⁹	0.47/1.42	–	eGFP/*PSA assay in LNCaP cells

Abbreviations: AF-2, activation function 2; AR-WT, wild-type androgen receptor; eGPF, enhanced green fluorescent protein.

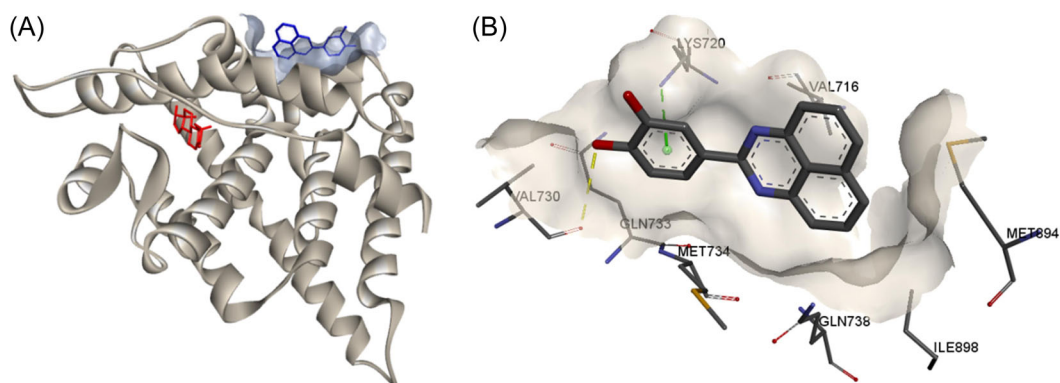


FIGURE 4 Compound 5 situated at activation function 2 (AF-2). (A) Full protein, testosterone (red), AF-2 and compound 5 (blue); (B) AF-2 binding site, hydrogen bonding (yellow), cation- π interaction (green). [Color figure can be viewed at [wileyonlinelibrary.com](https://onlinelibrary.wiley.com/doi/10.1002/mr.21961)]

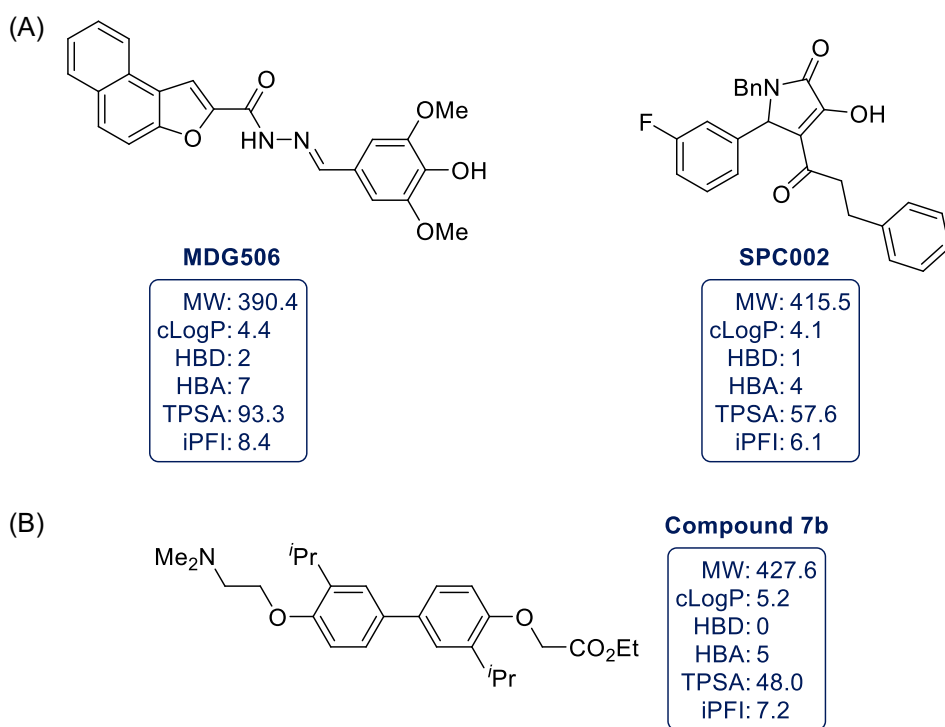


FIGURE 5 (A) Activation function 2 (AF-2) antagonists identified via virtual screening and quantitative structure-activity relationship; (b) biaryl AF-2 inhibitor reported by Weiser et al. cLogP, calculated lipophilicity coefficient; HBA, hydrogen bond acceptor; HBD, hydrogen bond donors; iPFI, intrinsic property forecast index; MW, molecular weight; TPSA, topological polar surface area.

additional optimization to replace the undesired moiety, and instead utilize the series as a mechanistic tool.⁶¹ Of the diarylhydrazide series, **MDG506** displayed the lowest cytotoxicity, with cell viability of 80% at 50 μ M. Subsequent use of their designed hydrazide library, coupled with published data relating to non-LBP AR inhibitors, enabled the authors to identify the structurally novel non-LBP AR antagonist **SPC002** from the SPECS database via the use of

molecular topology-derived quantitative structure–activity relationship (SAR).^{51,52} **SPC002** displayed a comparable IC_{50} of 24 μ M and molecular dynamics and docking studies predicted **SPC002** to have a higher affinity for AF-2 than for binding function 3 (BF-3) of the AR, *vide infra*.⁵¹

MDG506 combines several aromatic rings which despite the presence of a number of polar groups, gives the molecule an overall high iPFI. Incorporation of further heteroatoms into the tricyclic aromatic motif could reduce the high iPFI, thereby improving the pharmacodynamic profile of **MDG506**. The presence of a hydrazide, a known toxicophore, may also present future toxicity concerns. **SPC002** consists of a comparatively more flexible scaffold, along with three minimally functionalised phenyl rings. This gives rise to a high cLogP with a low TPSA, and potential for promiscuous off-target effects. Future optimization could focus on the incorporation of heterocycles to tune logP, increased rigidity, and higher degrees of saturation to increase sp^3 character.

Biaryl PPI inhibitors have been identified and evaluated against both the ER α and AR. These compounds were designed to antagonize the binding of coactivator proteins to the receptor coactivator binding domain. Compound **7b** exhibited significant AR inhibition at concentrations of ≤ 40 μ M and was the only analog reported to possess selectivity for the AR with reliable cell viability (Figure 5B).⁵³ Various substitution patterns on the biaryl linker resulted in cytotoxicity at concentrations above 50 μ M. Further exploration of the SAR has solely focused on activity against ER α .⁶²

Compound **7b** has a high cLogP value, 12 rotatable bonds, and an iPFI > 7 . Considering the presence of a basic amine and its comparatively high lipophilicity, the molecule is likely to exhibit off-target liabilities, demonstrated by the cytotoxicity of structurally related analogs. In addition to this, the presence of a basic tertiary alkyl amine and an aromatic core indicates a potential alert for hERG channel inhibition and associated cardiotoxicity.⁶³

Ravindranathan et al. designed compound **D2** to mimic the leucine-rich motifs, LXXLL of proteins that bind to AF-2 (Figure 6A). Compound **D2** was shown to disrupt the interaction between the AR and coregulator PEPL1 and inhibit AR-mediated prostate cancer cell proliferation, both with an IC_{50} of 40 nM.⁵⁴ Furthermore, compound **D2** demonstrated cytostatic effects in xenograft prostate tumors *in vivo* and cultured human tumors *ex vivo*. Subsequent SAR exploration afforded compound **14d**, which demonstrated higher antiproliferative activity with an IC_{50} of 16 nM against LNCaP cells and similar efficacy in the PEPL1 displacement assay.⁵⁵

The cLogP and iPFI values of compound **D2**, combined with the presence of polar functional groups suggest an acceptable profile in relation to absorption considering solubility and permeability. This profile is improved upon in the case of compound **14d** because replacing the methyl ester with a carboxamide affords an improved cLogP and likely imparts a degree of solubility. Unfortunately, the presence of a nitro group is a potential liability as the moiety is known to undergo metabolism to nitroso compounds and hydroxylamines which are toxicophores and anilines which are often genotoxic.^{64,65}

Johnston et al. recently described the development of a fluorescence-based bioassay for a high-throughput screening (HTS) campaign of novel inhibitors of AR-coactivator PPIs, specifically AR-TIF2.⁵⁶ Using the Library of Pharmacologically Active Compounds (LOPAC) to test this assay, five nonsteroidal compounds were identified to inhibit DHT-induced AR-TIF2 PPIs with IC_{50} values ranging from 0.56 to 1.17 μ M including **TPCK** and **Parthenolide** (Figure 6B).

Despite relatively suitable physicochemical properties, **TPCK** is likely to be highly promiscuous due to the presence of an activated α -chloroketone functionality and hence, prone to covalent bonding to a broad range of proteins. **Parthenolide** possesses no HBD and has a very low TPSA which will likely confer poor solubility and makes absorption a potential issue. The compound also possesses a Michael acceptor and an epoxide moiety, making promiscuous binding to off-target proteins through covalent modification, a potential concern. While the identified hits are far from lead-like, the authors noted the small and outdated nature of the LOPAC library and subsequently screened a larger, more diverse compound deck.⁶⁶ Of the 286 confirmed active compounds, approximately 60% were able to inhibit or disrupt AR-TIF2 PPIs with an $IC_{50} < 40$ μ M.⁶⁷ Johnston et al. have since reported the development of five assays that target the AF-2 domain, although the structures of the hits have not been disclosed to date.⁶⁸

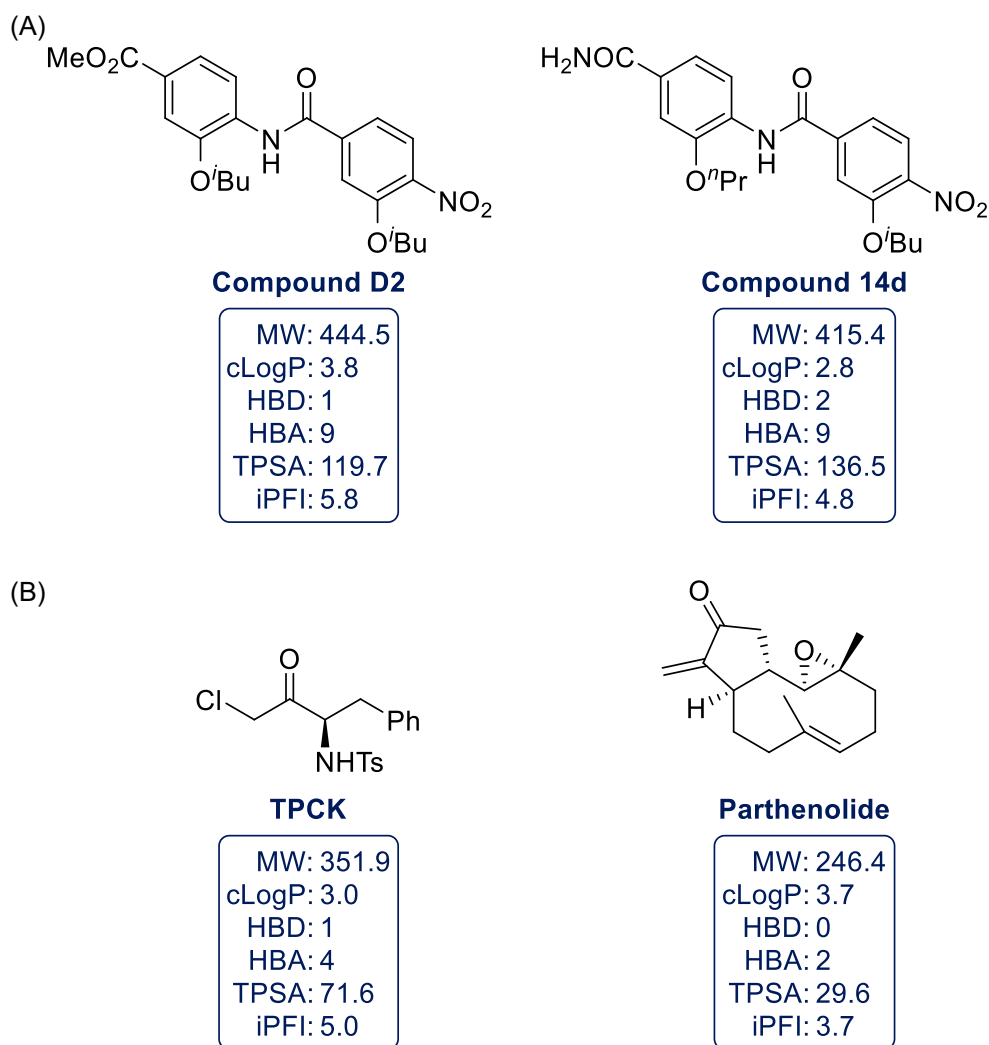


FIGURE 6 (A) Benzamide α -helix mimetic activation function 2 (AF-2) inhibitors; (B) novel AF-2 inhibitors TPCK and parthenolide identified via a novel bioassay targeting the interaction between the AR and TIF2. cLogP, calculated lipophilicity coefficient; HBA, hydrogen bond acceptor; HBD, hydrogen bond donors; iPFI, intrinsic property forecast index; MW, molecular weight; TPSA, topological polar surface area. [Color figure can be viewed at [wileyonlinelibrary.com](https://onlinelibrary.wiley.com/terms-and-conditions)]

More recent work has utilized computational modeling to screen the ZINC database for chemical entities that interact with the AR AF-2. This led to the synthesis of an oxadiazole series of which **LHJ-647** was the most potent (Figure 7A).⁵⁷ **LHJ-647** disrupted the interaction between AF-2 and the coactivator RIPK1 and, it also suppressed AR transcription in AR-transfected PC-3 cells with an IC_{50} of $\sim 1 \mu M$.

LHJ-647 is a small compound with modest lipophilicity furnished with a balance of polar groups that observes Lipinski's rules and possesses a favorable iPFI value. This indicates an acceptable developability profile and potential for further optimization. One particular feature of note is the embedded aniline, which as previously acknowledged, has the potential to be associated with genotoxicity.

Recently, Liu et al. have developed a pharmacophore model based on structures of the AR with AF-2 bound small molecules available from the Protein Data Bank database.⁵⁸ This model was used to conduct a virtual screen

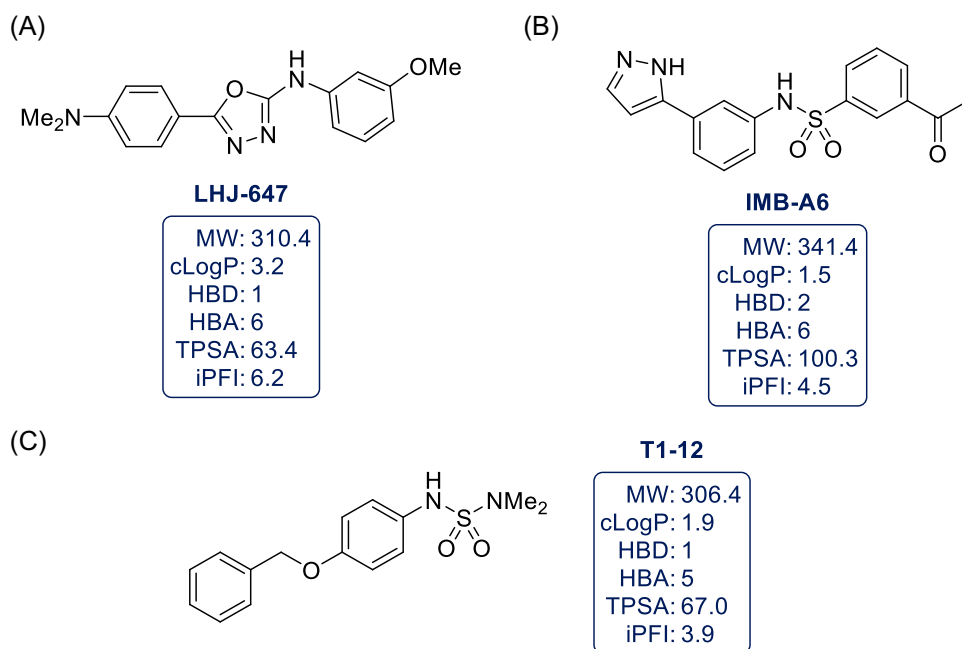


FIGURE 7 (A) Activation function 2 (AF-2) inhibitor **LHJ-647**, the most potent member of an oxadiazole series identified via computational modeling; (B) **IMB-A6**, identified via a pharmacophore model derived from Protein Data Bank structures of AF-2 binders; (C) **T1-12**, identified in a small structure–activity relationship study following a virtual screen. cLogP, calculated lipophilicity coefficient; HBA, hydrogen bond acceptor; HBD, hydrogen bond donors; iPFI, intrinsic property forecast index; MW, molecular weight; TPSA, topological polar surface area. [Color figure can be viewed at wileyonlinelibrary.com]

of the ZINC database and identified **IMB-A6**, which inhibited AR-WT activity in LNCaP and AR-transfected PC-3 cells with an IC_{50} of 10 μ M (Figure 7B). **IMB-A6** also inhibited clinically relevant AR mutants; T877A, W741L, and F876L in PC-3 cells. A library of 248 chemically similar analogs was screened and 14 compounds were selected to be tested against the same AR mutants. Eight of the compounds retained modest activity at 10 μ M concentration, validating the efficacy of the chemotype represented by **IMB-A6**. The low MW and cLogP, accompanied by a good iPFI score and balance of functionality make **IMB-A6** an attractive compound with likely potential for further development, although the embedded ketone represents a potential metabolic liability.

Recently, Chai et al. employed a structure-based virtual screen followed by SAR exploration of the sulfonamide moiety to identify a series exemplified by **T1-12** (Figure 7C).⁵⁹ The most potent analog, **T1-12** effectively displaced coactivator peptides from the AF-2 pocket and displayed AR transcriptional inhibition with an IC_{50} of 0.47 μ M in LNCaP cells. **T1-12** also inhibited tumor growth by 65% in xenograft models at a dose of 2.5 mg/kg/week when administered intratumorally.

T1-12 has a desirable *in silico* developability profile, displaying a low MW, cLogP, and TPSA. The favorable iPFI score combined with the balance of polar and nonpolar functionality makes it an acceptable candidate for a more thorough SAR exploration of the surrounding chemical space.

The developability profile of each of the compounds discussed in this section can be summarized by applying three main parameters (MW, cLogP, and iPFI) relating to solubility and permeability (absorption), along with important considerations (TPSA, rotatable bonds, HBD, and HBA). In addition, to avoid toxicity and promiscuous off-target binding, a low MW and cLogP are desirable.⁶⁹ In summary, **Parthenolide**, **TPCK**, compound **4**, **T1-12**, **LHJ-647**, compound **6**, and **IMB-A6** all maintain low MW, and acceptable cLogP and iPFI values (Figure 8). In terms

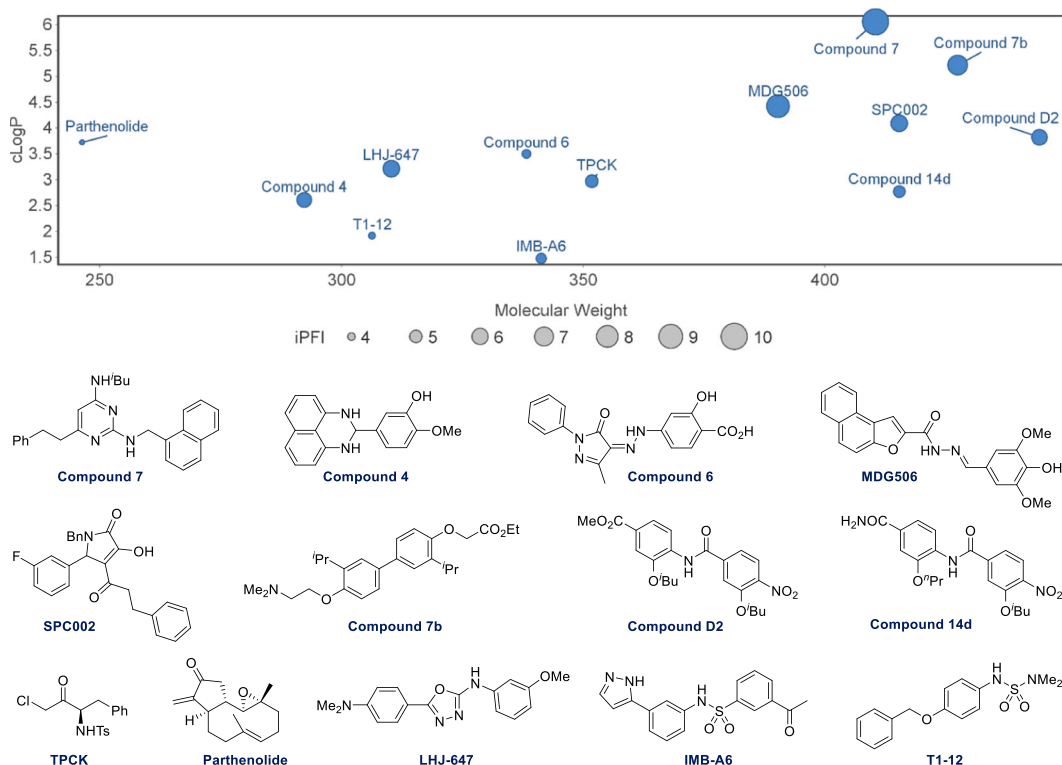


FIGURE 8 Developability overview of compounds that target the activation function 2 domain. [Color figure can be viewed at wileyonlinelibrary.com]

of structural alerts, **Parthenolide** has a Michael acceptor and an epoxide which are not considered to be optimal for further drug development. Having stated this, Michael acceptors and other covalent inhibitors are increasingly viewed as being acceptable in, for example, oncology applications.⁷⁰ **TPCK** and **SPC002** are likely to be involved in Nonspecific covalent binding. Compound **7** has a high cLogP value >5 which could lead to off-target effects. Compound **6**, **MDG506**, and compounds **D2** and **14d** displayed general cytotoxicity which can be ascribed to the hydrazide and nitro moieties, respectively. Compound **7b** has a potential hERG issue through the basic tertiary amine. From consideration of physicochemical properties, reported potency for AR inhibition, and the presence of structural alerts, our analysis indicates that **LHJ-647**, **IMB-A6**, and **T1-12** are optimal starting points for the future development of AF-2-directed AR inhibitors.

4 | BF-3-TARGETING COMPOUNDS

In pursuit of new AR AF-2 binders, Estébanez-Perpiña et al. identified a novel surface binding site termed BF-3, which displayed allosteric activity for AF-2.⁷¹ In addition, Nonspecific AF-2/BF-3 binders were reported, including **TRIAC** and **Tolfenamic acid** (Figure 9A). These compounds disrupted coactivator SRC2 binding with IC₅₀ values of ~50 μ M (Table 3) and inhibited AR activity in a dose-dependent manner in the 10–30 μ M range in vitro, serving as proof of principle for receptor inhibition via BF-3.

Both compounds present a common pharmacophore and are similar in terms of the developability profiles. The three iodine atoms present in **TRIAC** dramatically increase the MW; however, there is potential for exploring

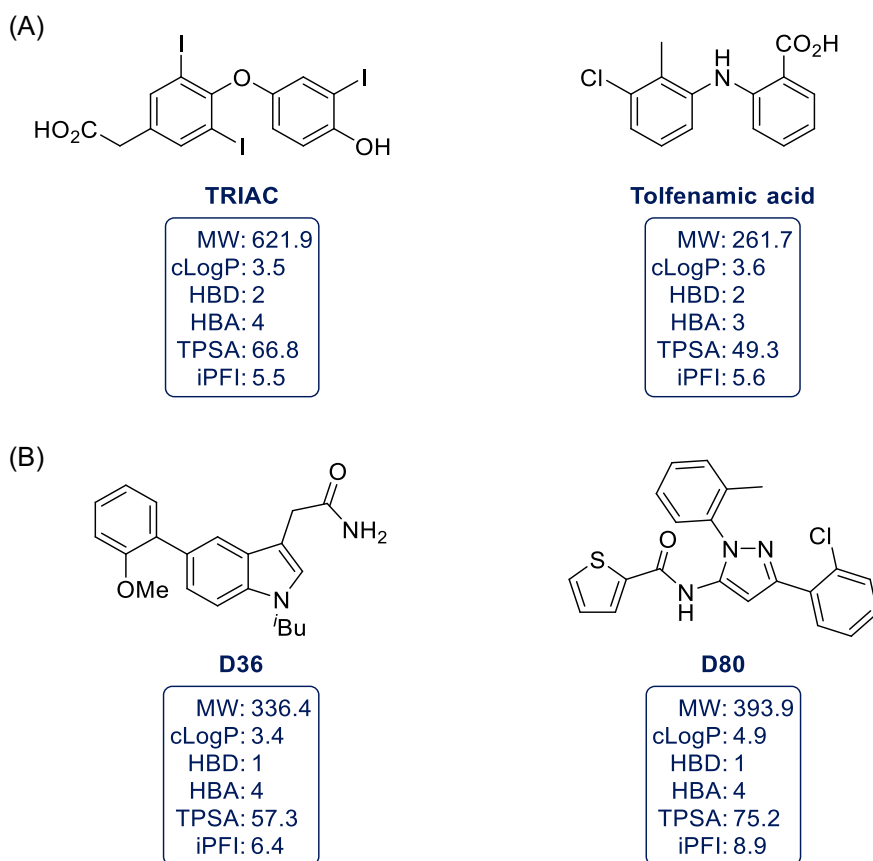


FIGURE 9 (A) Nonspecific binders of activation function 2 and binding function 3; (B) hits identified via a conformation-based assay. cLogP, calculated lipophilicity coefficient; HBA, hydrogen bond acceptor; HBD, hydrogen bond donors; iPFI, intrinsic property forecast index; MW, molecular weight; TPSA, topological polar surface area. [Color figure can be viewed at wileyonlinelibrary.com]

alternative substitution patterns to alter the properties of the compound. **Tolfenamic acid** is a marketed pharmaceutical that inhibits the COX pathway.⁷⁹

Joseph et al. exploited the interaction between the AR and cofactor gelsolin to develop an assay for identifying small molecules that induce inactive conformations of the AR.⁷² This conformation-based assay identified two compounds **D36** and **D80** (Figure 9B). **D36** was the most potent, allosterically competing with the synthetic androgen, R1881 with an IC_{50} of 10 μ M. These compounds were reported to bind an AR surface site, which was proposed to be BF-3, and essentially induce a conformation similar to that of the unoccupied receptor. **D36** inhibited PSA transcription and proliferation in LAPC4 cells, as well as reducing proliferation in two CRPC cell models, SRAR LNCaP and VCaP.

Both compounds possess multiple aromatic rings which impact the iPFI, making solubility a potential concern. **D80** has a particularly high cLogP which consequently impacts iPFI, also the thiophene moiety can be prone to oxidation and metabolic instability.⁸⁰ The considerations make **D36** the more developable compound in terms of the available metrics, the core indole scaffold is also a well-known pharmacophore that offers potential for SAR exploration and further optimization.

The Cherkasov group has reported improvements to the modest potency and selectivity of BF-3-targeting antiandrogens.^{49,73} Virtual screening efforts followed by cellular assays afforded 55 hits (>50% inhibition at 50 μ M

TABLE 3 Inhibitory activity and assay description of BF-3 targeting compounds.

Compound	Reported activity AR–IC ₅₀ (μM)	Assay description
TRIAC ⁷¹	59	Fluorescence polarization assay for SRC2-3 displacement
Tolfenamic acid ⁷¹	47	Fluorescence polarization assay for SRC2-3 displacement
D36 ⁷²	10	Whole-cell-competition binding assay in VCaP cells
D80 ⁷²	34	Whole-cell-competition binding assay in VCaP cells
3 ⁷³	13.1	eGFP assay in LNCaP cells
4 ⁷³	38.8	eGFP assay in LNCaP cells
ZINC13574823 ⁷³	0.9	eGFP assay in LNCaP cells
54 ⁷⁴	1.5	eGFP assay in LNCaP cells
	1.6/6.4*	PSA expression assay in LNCaP cells/*MR49F cells
18 ⁷⁵	0.7	eGFP assay in LNCaP cells
	0.84/2.18*	PSA expression assay in LNCaP cells/*MR49F cells
	0.55/1.31*	MTS cell proliferation assay in LNCaP cells/*MR49F cells
23 ⁷⁶	0.31	eGFP assay in LNCaP cells
	0.21/6.02*	PSA expression assay in LNCaP cells/*MR49F cells
	0.71/2.01*	MTS cell proliferation assay in LNCaP cells/*MR49F cells
	6.1/7.51*	Fluorescence polarization assay for Bag1L displacement vs AR-WT/* vs AR-T877A mutant
VPC-13566 ⁷⁷	0.05	eGFP assay in LNCaP cells
	0.08/0.35*	PSA expression assay in LNCaP cells/*MR49F cells
	0.15/0.07*	MTS cell proliferation assay in LNCaP cells/*MR49F cells
	1.73	pARR3-tk-luciferase assay in PC-3 cells vs. AR-WT
	0.10–13.40	pARR3-tk-luciferase assay in PC-3 cells vs. 24 different AR mutants
VPC-13789 ⁷⁸	0.19	eGFP assay in LNCaP cells
	0.52	PSA expression assay in LNCaP cells after 3 days of treatment
VPC-13822 ⁷⁸	0.66	PSA expression assay in LNCaP cells after 3 days of treatment

Abbreviations: BF-3, binding function 3; eGPF, enhanced green fluorescent protein.

by eGFP assay) including compound 3, compound 4, and ZINC13574823 (Figure 10). The most potent of these hits demonstrated AR transcriptional IC₅₀ values ranging from 0.9 to 50 μM. Mechanistic action via AF-2 or the LBP was disproved via SRC2 and DHT displacement assays, respectively.

Compound 3 has both a high cLogP and iPFI; it is likely that these characteristics will lead to low solubility and possible off-target effects. In addition, the ether chains have the propensity to be rapidly metabolized. Compound 4 possesses a number of rotatable bonds and consists of two catechol moieties, which are pan-assay interference (PAINS) structural alerts that are known to yield false positives.^{81,82} ZINC13574823 has a high cLogP and a low TPSA, which combined with a lack of polar groups could again lead to concerns over solubility and off-target

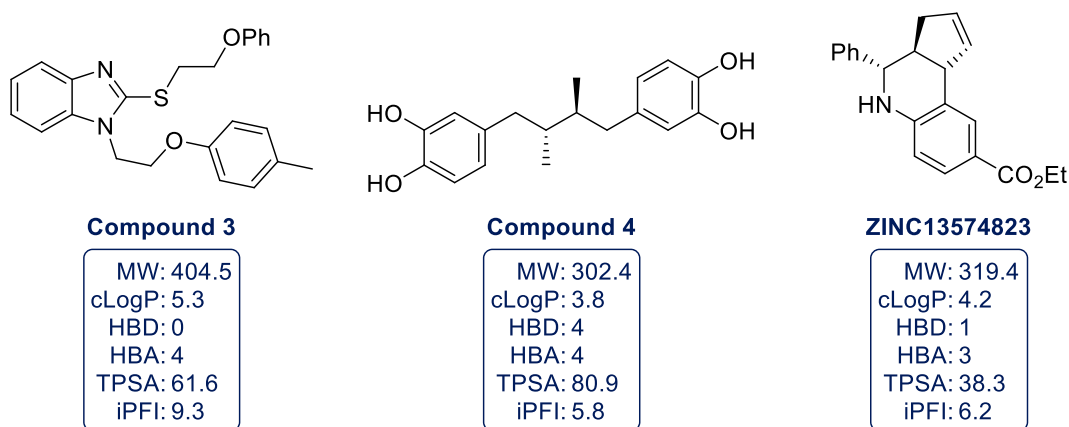


FIGURE 10 Binding function 3 targeting hits identified in a virtual screening campaign. cLogP, calculated lipophilicity coefficient; HBA, hydrogen bond acceptor; HBD, hydrogen bond donors; iPFI, intrinsic property forecast index; MW, molecular weight; TPSA, topological polar surface area. [Color figure can be viewed at wileyonlinelibrary.com]

effects. From a biostructural perspective, compounds **3** and **4** have been confirmed through X-ray crystallography to bind the AR BF-3 (Figure 11).⁷³

A thorough SAR exploration of compound **3** led to the identification of compound **54**, compound **18**, compound **23**, and **VPC-13566**, accompanied by sequential increases in potency in the variety of assays employed, see Table 3 *vide infra* (Figure 12).^{74–77} Ultimately, the studies found **VPC-13566** to be a selective BF-3 inhibitor with nanomolar potency in multiple assays against both AR-WT and a range of clinically relevant mutants. In addition, **VPC-13566** also reduced PSA expression and cell viability of enzalutamide-resistant MR49F cells and reduced PSA expression and tumor volume at levels comparable with **enzalutamide** in a castration-resistant xenograft model.

Compounds **54** and **18** broadly occupy drug-like space in terms of Lipinski's rules. Further optimization led to compounds **23** and **VPC-13566**, which possess a higher cLogP and iPFI and lower MW, however, are accompanied by significant increases in potency, Table 3 (*vide infra*).

Most recently, Leblanc et al. conducted a pharmacokinetic optimization of **VPC-13566**, which despite its potent activity in vivo, suffers from metabolic instability.⁷⁸ Efforts to circumvent this led to the development of **VPC-13789**, which demonstrated a significant improvement in microsomal half-life from 21 to 206 min, whilst maintaining an IC₅₀ of <200 nM (Figure 13). In an androgen displacement assay, **VPC-13789** had no effect at 10 μM concentration, discounting a mechanism that functions via the LBP; furthermore, **VPC-13789** had no effect on the growth of AR-negative PC-3 cells, indicating mechanistic targeting of the AR. Due to high peak plasma concentration and rapid clearance, the authors subsequently developed **VPC-13822**, a methylenephosphate prodrug (Figure 13). **VPC-13822** inhibited PSA expression in LNCaP cells with a similar IC₅₀ to the parent compound 0.66 and 0.52 μM, respectively. It underwent steady conversion to the parent drug with a half-life of 2 h, and significantly reduced tumor growth in a xenograft model.

The pharmacokinetic parameters for **VPC-13789** remain largely similar to the other members of the series, and while the metabolism issue was addressed, it still exhibited a cLogP close to the recommended upper limit of Lipinski's rules and accordingly a high iPFI value. This was successfully addressed utilizing a prodrug strategy, with a significant drop in cLogP and iPFI being reflected by a twofold increase in solubility. Notably, **VPC-13822** demonstrated no significant signs of toxicity over the 4-week xenograft study following a per oral (po) dose of 115 mg/kg twice daily. The relatively high MW of **VPC-13822** violates Lipinski's rule; however, Protti et al. recently

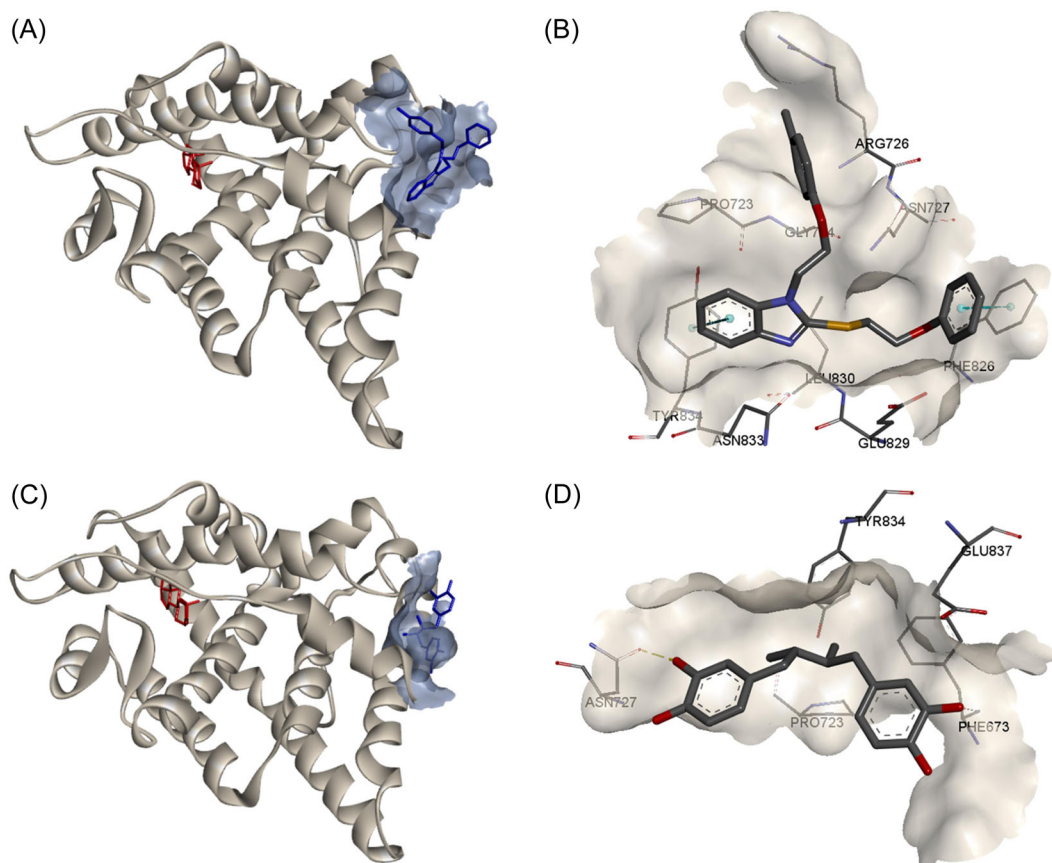


FIGURE 11 Compounds **3** and **4** situated at binding function 3 (BF-3). (A) Full protein, testosterone (red), BF-3 and compound **3** (blue); (B) BF-3 binding site, π - π interaction (cyan) (PDB:2YLO); (C) full protein, testosterone (red), BF-3, and compound **4** (blue); (D) BF-3 binding site, hydrogen-bonding (green) (PDB:3ZQT). [Color figure can be viewed at [wileyonlinelibrary.com](https://onlinelibrary.wiley.com/doi/10.1002/mr.2061)]

recommended an expansion of widely used parameters that determine drug-like space, based on the prevalence of orally bioavailable prodrugs and natural products that exceed the existing guidelines.⁸³

All of the BF-3 targeting compounds comply with Lipinski's rules, except for compound **3**, **TRIAC**, and the prodrug, **VPC-13822** (Figure 14). Compounds **54** and **18** have the most favorable developability profile; their substantial optimization to **VPC-13789** has resulted in the lead **VPC-13822** which has a good cLogP and iPFI, a reasonable HBD/A count, and TPSA, with the methylenephosphate group attributing to the high MW. Compound **D80** contains thiophene which is potentially metabolically unstable. Compound **D36**, however, displays a moderate cLogP and MW and has been underexplored in terms of SAR, presenting an opportunity for future development. Compound **4**, unfortunately, contains a number of rotatable bonds and also known structural alerts for PAINS. **ZINC13574823** has a novel structural scaffold with desirable sp^3 character and a high degree of potency for an initial hit; however, the comparatively high cLogP and low TPSA pose potential issues that would require addressing via the introduction of polar functionality.^{84,85}

Targeting AF-2 and BF-3 are evidently valid approaches toward novel CRPC treatments; however, this is only possible in cases where the LBD is retained (i.e., no splice variants which lack the LBD). Unfortunately, this approach fails to provide viable treatments to patients suffering from AR mutations that circumvent the inhibition of the different LBD regions. Consequently, a multi-targeted approach considering other regions of the AR is crucial to achieving improved outcomes for CRPC patients.

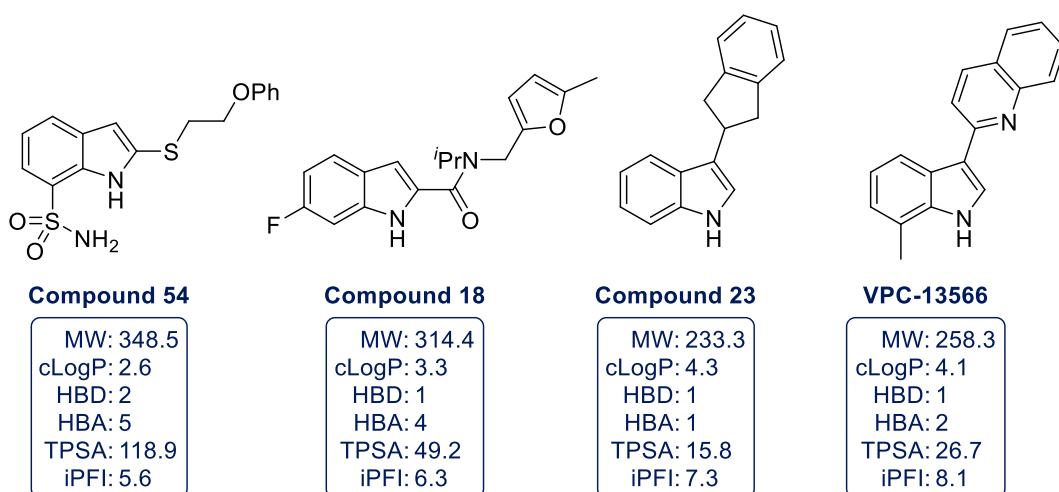


FIGURE 12 VPC compounds identified via structure–activity relationship exploration. cLogP, calculated lipophilicity coefficient; HBA, hydrogen bond acceptor; HBD, hydrogen bond donors; iPFI, intrinsic property forecast index; MW, molecular weight; TPSA, topological polar surface area.

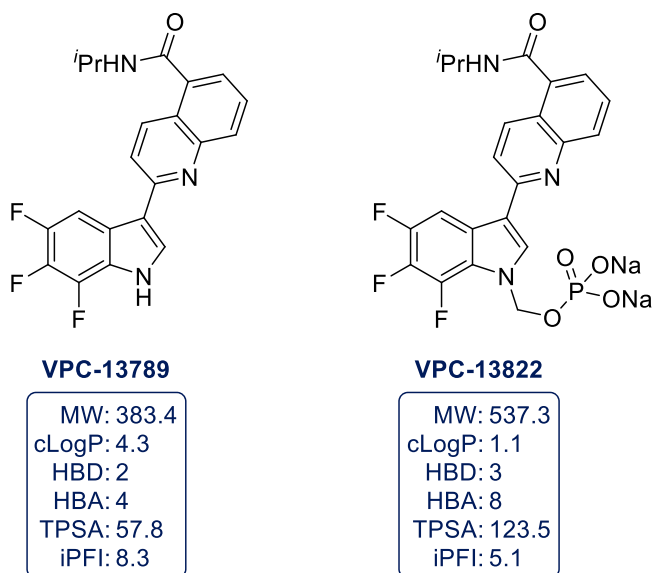


FIGURE 13 Optimization of VPC-13566 ADME properties to afford VPC-13789 and a prodrug analog. cLogP, calculated lipophilicity coefficient; HBA, hydrogen bond acceptor; HBD, hydrogen bond donors; iPFI, intrinsic property forecast index; MW, molecular weight; TPSA, topological polar surface area. [Color figure can be viewed at [wileyonlinelibrary.com](https://onlinelibrary.wiley.com/terms-and-conditions)]

5 | TARGETING THE NTD

Deletion studies involving the NTD have demonstrated that it is essential for receptor function, making it as appealing as it is challenging as a drug target. A raft of data indicates that the NTD is required for transcription, and is present in all forms of the AR, including the range of known mutants and splice variants.⁸⁶

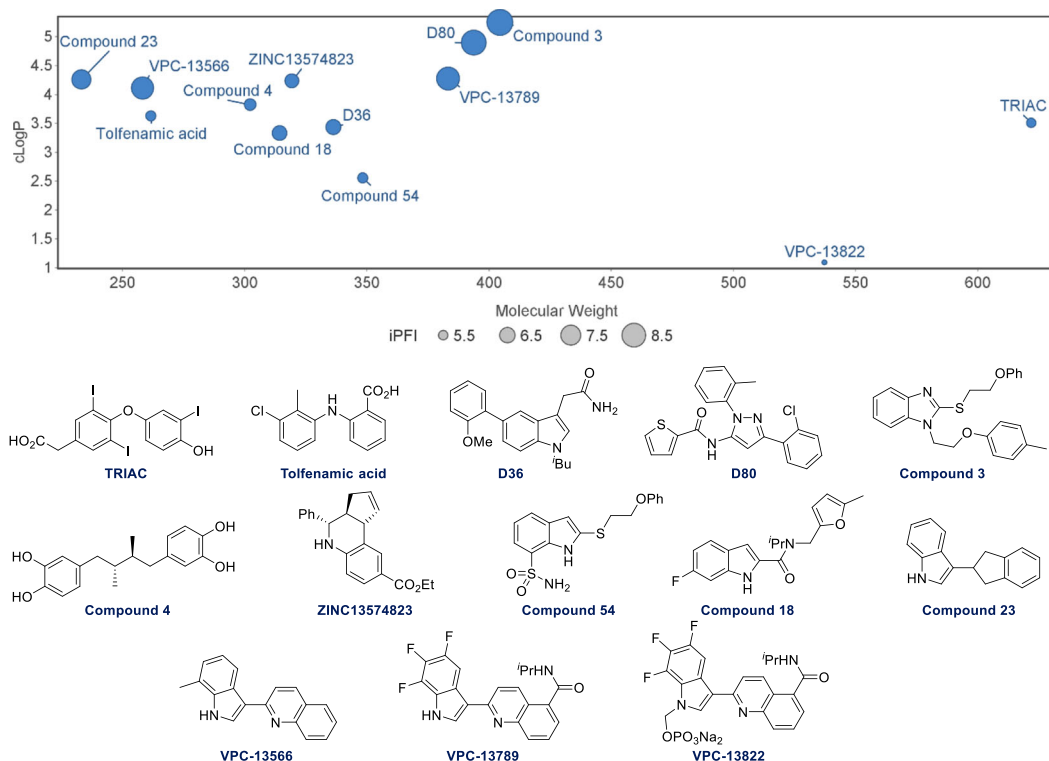


FIGURE 14 Developability overview of compounds that target the binding function 3. [Color figure can be viewed at [wileyonlinelibrary.com](https://onlinelibrary.wiley.com/doi/10.1002/mr.2061)]

Based on this, it is anticipated that treatments targeting the NTD would provide efficacy against AR variants resistant to current treatments formed from alternative splicing, for example, enzalutamide-resistant F876L and AR-Vs lacking the LBD. The main challenge of this approach is developing drugs that would target the intrinsically disordered domain, which is not amenable to Structure-Based Drug Design.⁸⁷ It has been proposed that the disorder of the NTD might allow it to act as a center for signaling pathways via PPIs with coactivators of varying sizes, adopting different conformations for each.^{88,89} Recent cryoelectron microscopy studies have elucidated the structure of the AR dimer complexed with DNA and coactivators p300 and SRC3. In this study, antibody labeling occurred with differing efficiency for the two NTDs of the dimer, substantiating the proposal that distinct NTD conformations result in differences in coactivator recruitment.⁹⁰ Computational methods are beginning to emerge for the rational design of drugs that target intrinsically disordered proteins and have been recently reviewed.⁹¹ However, it is a contemporary research area, and more experience is required before its utility can be fully established.

Mutations occur proportionately across the whole AR and the NTD is no exception; 10% of its residues have the potential for mutation in prostate cancer.⁹² Results from our laboratories demonstrated that NTD-mutations generally produce a loss of function or no significant difference compared to AR-WT, with only a minority leading to a constitutive gain of function. Nevertheless, mutations with no apparent change in WT activity have been proposed to drive cancer progression via other routes such as altered binding to coregulators, increased protein stability, and gene amplification, which suggests that various NTD mutations can influence the progression of CRPC.⁹³

The development of drugs that target the NTD has garnered much attention in recent years, largely due to the discovery of AR-Vs.^{20,22,94–97} Although this topic has been reviewed previously, we intend to address both attempts to target the NTD pharmacologically and appraise the capacity of natural products identified as pharmaceutical leads.

5.1 | NTD-targeting natural products

Natural products are an abundant source of bioactive compounds and potential innovative drug leads, evidenced by the fact that they account for more than 40% of all pharmaceuticals on the current market.^{98–100} In addition to this, approximately half of the available cancer therapies also originate from natural products.^{101,102}

In 2008, Sadar et al., isolated **sintokamides A–E** and **dysamide A** (Figure 15A) from the marine sponge *Dysidea* sp. collected near Palau Sintok, Indonesia.¹⁰³ The **sintokamide** family is a group of polychlorinated marine peptides derived from chlorinated leucine and were the first small molecules shown to inhibit the AR via the NTD.

Sintokamide A was shown to inhibit forskolin-induced transactivation of the AR-NTD when pretreated at 5 μ M for 1 h via a luciferase reporter assay.¹⁰³ Furthermore, **sintokamide A** exhibited an AR transcriptional IC₅₀ of 10 μ M and antiproliferative IC₅₀ of 35 μ M in LNCaP cells. **Dysamide A** and **sintokamides B, C, and E**, also displayed antiandrogenic activity at 5 μ g/mL in LNCaP cells determined by PSA-luciferase reporter gene assay.¹⁰⁴ Further analysis identified the AF-1 region in the NTD as the binding site for **sintokamide A** and selectivity over other hormone receptors was established. In addition, efficacy against both AR-FL and AR-Vs was demonstrated by utilizing luciferase and proliferation assays, as well as xenograft models.¹⁰⁵

Recently, Sadar and Anderson explored the SAR surrounding the **sintokamide** pharmacophore, using a PSA-luciferase assay to tune the potency.¹⁰⁶ It was established that transcriptional inhibition was proportional to the number of chlorine atoms present within the scaffold. Another modification was the replacement of the propionamide moiety at the *N*-terminus with a bulkier, more lipophilic *N*-pivaloyl group to afford the more potent synthetic analog **LPY36** (Figure 15A). During these studies, the synthesis of the scaffold was simplified via the removal of two of the four stereogenic centers, which had no effect on the antagonist profile. This was accompanied by a threefold increase in potency via luciferase assay and increased suppression of LNCaP cell proliferation.

Further investigation of the **sintokamide** family provided a beachhead for the development of NTD-targeting inhibitors. However, the core scaffold possesses a large degree of molecular flexibility, and the compounds have a high MW and cLogP which are likely indicative of poor developability properties such as solubility and permeability. From a DMPK perspective, this profile is problematic for the same reasons, with a number of metabolic hotspots evident in the **sintokamide** family. Furthermore, the activity requirement of multiple alkyl halides raises concerns about off-target effects, although these are anomerically stabilized. Having stated this, a comparatively lower (fourfold) selectivity of **LYP36** for AR-positive LNCaP over AR-negative PC-3 cell viability was observed, indicating the potential for off-target effects.

Meimetis et al. isolated **niphatenones A and B** from the marine sponge *Niphates digitalis* collected in Dominica, assessed their ability to inhibit AR transcription, and conducted an SAR study (Figure 15B).¹⁰⁷ The natural products were found to be the most potent compounds of the SAR study, with IC₅₀ values of approximately 5 μ M via two luciferase assays.¹⁰⁸ Interestingly, both enantiomers of **Niphatenone B** demonstrated comparable IC₅₀ values of 5.2 and 6.3 μ M.¹⁰⁸ However, the Michael acceptor displayed reactivity with glutathione, suggesting that in turn, this would lead to off-target binding and thus limiting its potential drug scaffold for further development.

The **niphatenone** compounds consist of an extensive aliphatic carbon chain which results in increased molecular flexibility and a higher than desirable cLogP. For these reasons, aqueous solubility is predicted to be poor with a likely high degree of plasma protein binding, allied with the potential for extensive metabolic oxidation. Most importantly, as a general thiol alkylating agent, off-target toxicity for these molecules is likely.

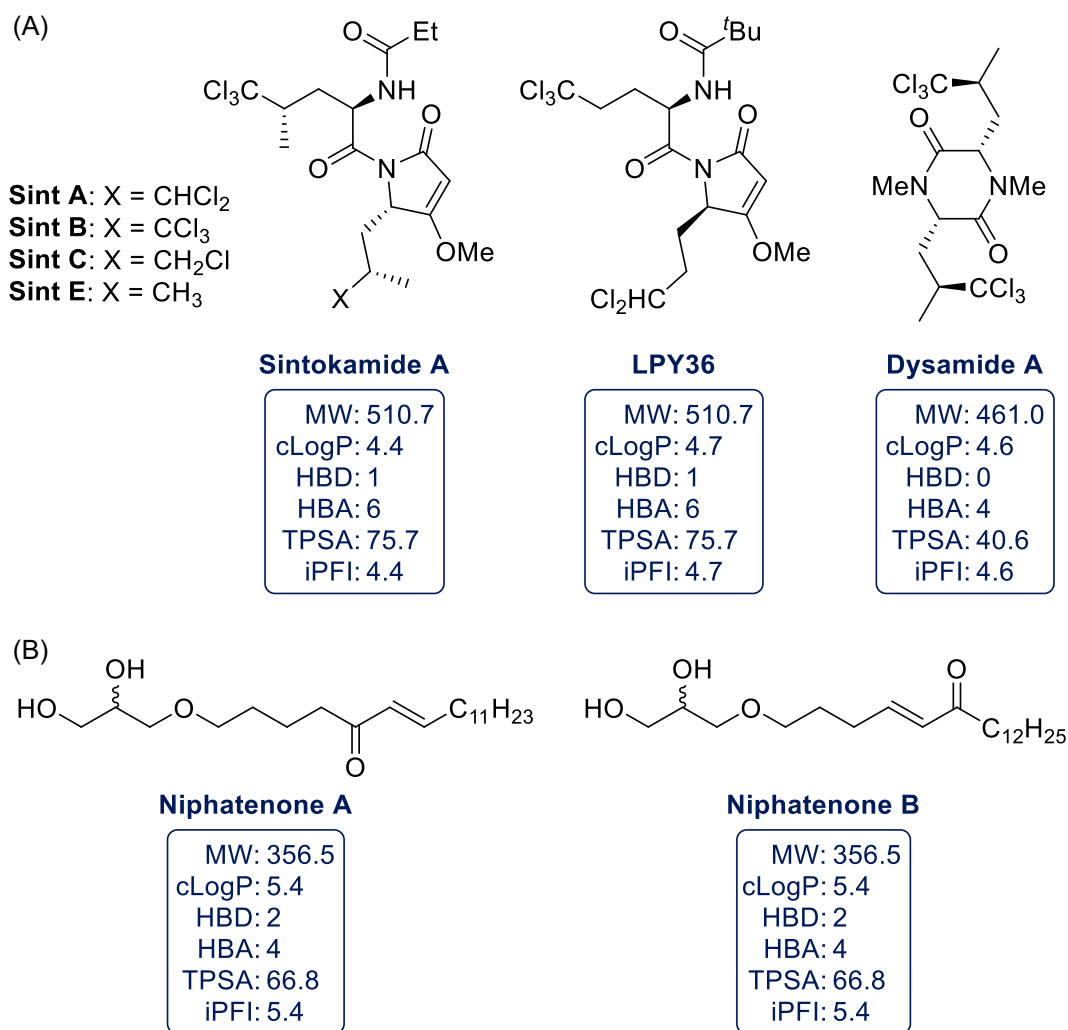


FIGURE 15 (A) Sintokamide family, synthetic analog LPY36, and Dysamide A; (B), NTD inhibitors Niphatenone A and B. cLogP, calculated lipophilicity coefficient; HBA, hydrogen bond acceptor; HBD, hydrogen bond donors; iPFI, intrinsic property forecast index; MW, molecular weight; TPSA, topological polar surface area. [Color figure can be viewed at [wileyonlinelibrary.com](https://onlinelibrary.wiley.com/terms-and-conditions)]

Mahanine is a carbazolidine alkaloid, isolated from *Murraya koenigii*, a curry leaf plant cultivated in Southeast Asia (Figure 16A).¹⁰⁹ **Mahanine** was also found to be present in the edible Thai vegetable *Micromelum minutum*, rendering it readily available.¹¹⁰ In terms of pharmacology, **mahanine** has been shown to inhibit DHT-induced transactivation of the AR in a dose-dependent manner in the 2.5–10 μ M range, assessed by ARR3-TK-luciferase and PSA-luciferase assays. Inhibition of ligand-independent transactivation was also demonstrated using a Gal4-DBD-AR-NTD fusion protein via luciferase assay; activity towards a protein construct with the DBD of the Gal4 transcription factor precludes a mechanism of action via the AR-DBD, providing evidence that inhibition functions through the AR-NTD.¹¹¹ In addition to direct inhibition of the AR, **mahanine** was reported to display other mechanisms of AR disruption, including enhanced ubiquitination which causes proteasomal degradation, inhibition of nuclear translocation, and reduction of phosphorylation at serine-81 due to suppression of CDK1 activity.

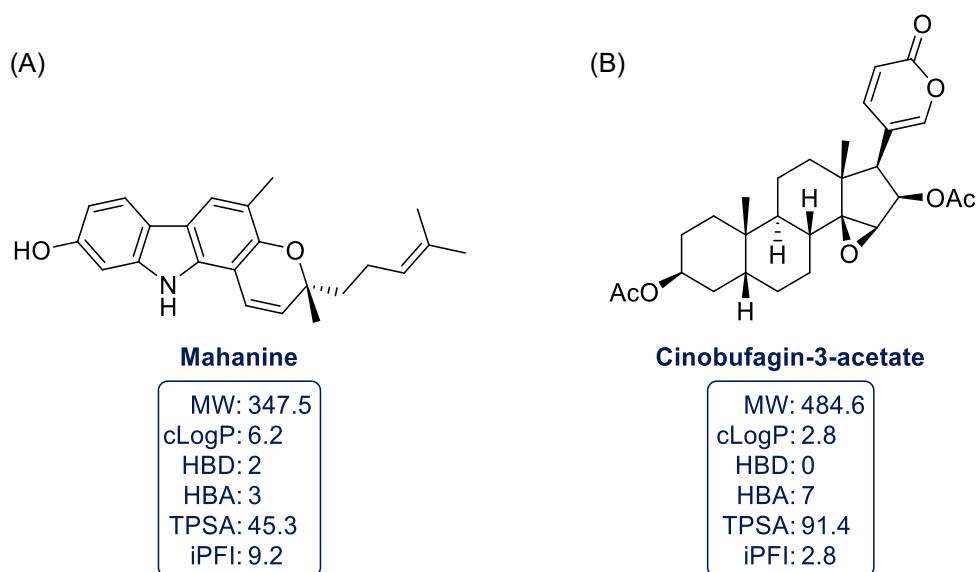


FIGURE 16 (A) Carbazole alkaloid, **mahanine**; (B) NTD-targeted inhibitor of the AR-STAT3 signaling pathway. cLogP, calculated lipophilicity coefficient; HBA, hydrogen bond acceptor; HBD, hydrogen bond donors; iPFI, intrinsic property forecast index; MW, molecular weight; TPSA, topological polar surface area. [Color figure can be viewed at wileyonlinelibrary.com]

Mahanine, exhibits a high cLogP and associated iPFI, indicative of poor solubility and risk of off-target effects. In addition, the phenol moiety is a likely site of phase II metabolism. Having stated this, the low MW of the compound potentially provides latitude for further development of the scaffold; the introduction of polar functional groups and replacement of the prenyl moiety could address the high cLogP and low TPSA.

Cinobufagin-3-acetate is a steroidal natural product secreted by the asiatic toad, *Bufo gargarizans* (Figure 16B).¹¹² Studies have shown that **cinobufagin-3-acetate** binds directly to the NTD thus inhibiting AR-STAT3 signaling—a pathway that is a key driver in the progression to CRPC.¹¹³ The compound demonstrated static levels of AR inhibition in the presence of varying concentrations of R1881, discounting a mechanism that functions via the LBP. **Cinobufagin-3-acetate** displayed significant inhibition against the clinical variants AR-V7 and ARv567es in LNCaP cells at concentrations of 1 and 10 μ M, respectively, and was found to reduce AR protein expression without altering AR mRNA levels or reducing AR nuclear translocation.

Cinobufagin-3-acetate exhibits a comparatively good cLogP for a steroidal lead, this is likely due to the presence of hydrophilic pyranone and acetate groups, which perhaps warrants further optimization of its pharmacokinetic profile, particularly against the background of the rich history of steroids as pharmaceutical agents. However, the epoxide moiety should be considered for possible nonspecific covalent interactions and consequently, potential off-target toxic effects.

5.2 | The EPI family

A library of compounds was isolated from the marine sponge, *Geodia lindgreni* by Sadar and Andersen in 2010 and are structurally similar to bisphenol A diglycidyl ether (**BADGE**).¹¹⁴ The collected library was then screened for its ability to block transactivation of the AR NTD, with **EPI-001** emerging as the most potent compound (Figure 17).

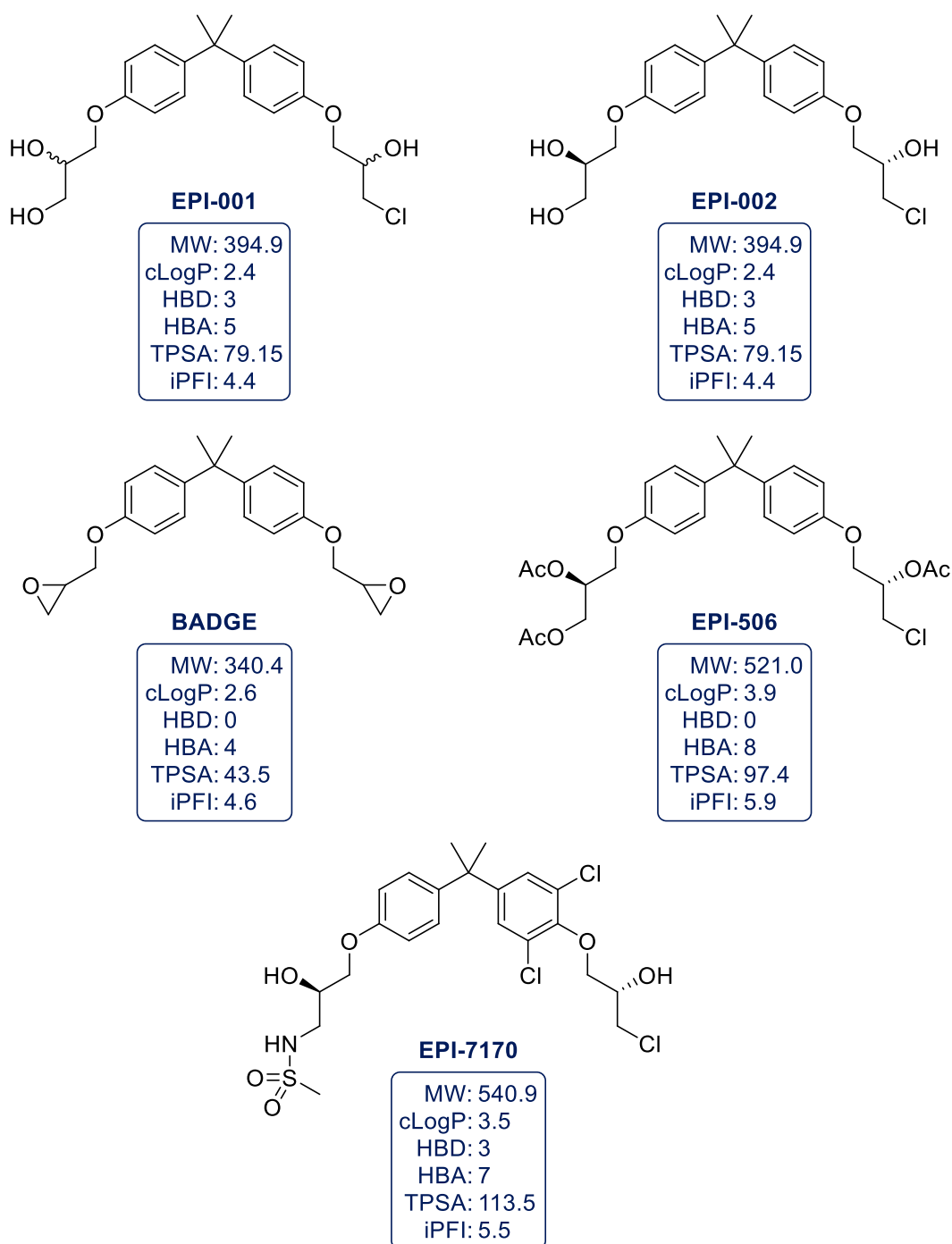


FIGURE 17 Early EPI analogs of BADGE, prodrug EPI-506, and next-generation analog EPI-7170. cLogP, calculated lipophilicity coefficient; HBA, hydrogen bond acceptor; HBD, hydrogen bond donors; iPFI, intrinsic property forecast index; MW, molecular weight; TPSA, topological polar surface area. [Color figure can be viewed at [wileyonlinelibrary.com](https://onlinelibrary.wiley.com/doi/10.1002/mr.22061)]

The compounds identified termed the EPI series, are derived from the racemic mixture **EPI-001**, and represent the most extensively investigated class of NTD inhibitor. **EPI-001** was initially shown to selectively block transactivation of the NTD via AF-1 and induce cytoerection of CRPC xenografts without overt toxicity at a dose of 50 mg/kg.¹¹⁴ EPI compounds display activity against truncated AR-Vs and require a chlorohydrin moiety to covalently bind to the AR, but do not possess nonspecific thiol alkylating abilities, as demonstrated with mercaptoethanol and glutathione.^{108,115} However, the chlorohydrin moiety is known to convert to the epoxide under neutral and basic pH, and **BADGE** is reactive to nucleophiles. **EPI-001** under acidic conditions did not form thiol adducts, but at pH 7.4 trace amounts of thiol adduct were observed, and at basic pH nearly complete conversion to the thiol adduct was noted.¹¹⁶ Placement of one of the hydroxy groups next to a basic site in the AF-1 pocket was proposed to facilitate the selective irreversible covalent binding. **EPI-002** (later termed ralaniten), a stereoisomer of **EPI-001** was evaluated via a luciferase assay to inhibit AR transcription with an IC₅₀ of 7.4 μM and oral administration at 200 mg/kg reduced the growth of VCaP xenografts.¹¹⁵

In more recent mechanistic studies, the interaction of **EPI-002** was localized to TAU-5 within the AF-1 region of the NTD, and it was shown to disrupt interactions between TAU-5 and essential coactivators CBP/p300 and RAP74.^{117,118} **EPI-002** has demonstrated efficacy against AR-V7 in LNCaP95 xenograft models, as well as AR mutant variants possessing gain-of-function mutations in either the LBD or the NTD.¹¹⁸ A clinical trial [NCT02606123] assessing **EPI-506**, an acetylated EPI prodrug, was initiated in 2015 but terminated two years later due to an excessive dose regimen (18 capsules per day).¹¹⁹

More recently, a next-generation analog, **EPI-7170** was reported to inhibit androgen-induced PSA-luciferase activity with an IC₅₀ of 1.1 μM (Figure 17).¹²⁰ **EPI-7170** has demonstrated inhibition of both AR-FL and truncated AR-Vs, which have been implicated in regulating DNA damage repair in prostate cancer.¹²¹ Accordingly, **EPI-7170** has been shown to sensitize AR-V-driven LNCaP95 cells to infrared radiation, increasing DNA damage and reducing cell survival and proliferation.

The effectiveness of the EPI series in combination with other therapeutics has also been demonstrated preclinically.¹²² Enhanced anticancer activity has been observed when combined with docetaxel, autophagy inhibitors, and the co-targeting of the AR and PI3K/Akt/mTOR pathways with mTOR inhibitor BEZ235.^{122–124} Most recently, **EPI-7170** has been combined with the CDK inhibitor palbociclib and the Pin1 inhibitor all-*trans* retinoic acid, with increased combination efficacy compared to monotherapy treatment observed in both cases in cell-based and xenograft models.^{125,126} A possible combination of EPI with **sintokamide A** has also been proposed, as the two compounds reportedly target separate sites in AF-1 and exhibit additive transcriptional inhibition.¹⁰⁵

A phase-1 clinical trial [NCT04421222] is currently underway exploiting the next iteration of the EPI scaffold, **EPI-7386** (structure undisclosed). **EPI-7386** displays improved metabolic stability and a 20-fold increase in potency compared to **EPI-002**.¹²⁷

The EPI family remains the most promising set of compounds for AR inhibition via the NTD and represents a potential new approach in the treatment of CRPC. Although the MW of some analogs exceeds 500 Da, the remaining parameters of the series are within a reasonable range. Potential concerns surrounding the alkyl halide moiety are minimal, as although it is essential for activity, the potential for nonspecific alkylation has been considered. Off-target effects of the series have been explored, as **EPI-002** has been shown to increase the transcription of metallothionein genes, driven by the transcription factor MTF-1. However, this effect was not observed for contemporary analogs in the EPI series and had no impact on AR inhibition.¹²⁸ Furthermore work by Brand et al. invokes nonselective action of **EPI-001** at much higher concentrations than previously employed to inhibit AR which suggests PPARγ as a target.¹¹⁶ Concerning toxicity, **EPI-002** has been examined in xenograft models up to a dose of 200 mg/kg, with only minor body weight loss observed indicating the minimal potential for toxicity.¹¹⁵ **EPI-7170** has also been assessed in murine models and induced no alteration in body weight at an efficacious dose of 30 mg/kg.¹²⁹ First-generation EPI analogs have a reported half-life of 3.3 h in mice and PK optimization led to the development of **EPI-7386** with a half-life of 24 h in humans.^{115,127}

Very recently, Asim and Spring reported the combination of two covalently linked AR inhibitors, **EPI-001** and **enzalutamide** (Figure 18).¹³⁰ The strategy was aimed at appending **enzalutamide** via the amide portion to the 1,2-diol of **EPI-001** through an epoxide opening maintaining the active chlorohydrin pharmacophore. Utilizing a biocompatible triazole with a PEG linker allowed different linker lengths to be investigated. This new class of hybrid compounds would simultaneously target the NTD and the LBD of the AR overcoming resistance to the standalone FDA-approved standard of care **enzalutamide**. Compounds **9a–e** were screened in a C4-2b prostate cancer cell line, known to express several AR-Vs in which **enzalutamide** possessed an LC₅₀ value of 63.5 μ M and **EPI-001** was slightly less potent at 84.8 μ M. In comparison, compounds **9a–9e** exhibited an 18–53 fold improvement with LC₅₀ values of 1.7–4.6 μ M. After further investigative biological studies, **9b** emerged as the lead compound. **9b** was shown to inhibit AR-mediated gene transcription in a luciferase assay and was able to significantly inhibit transcription of the PSA gene proving its direct engagement with the AR; furthermore, it produced negligible toxicity in PC-3 cells. The authors hypothesized that the improvement in cell toxicity was due to an entropic effect mediated by the linker which increases the local concentration of the second inhibitor that binds to the AR. The hypothesis is supported by studies whereby the dual inhibitors outperformed an equimolar concentration of **EPI-001** and **enzalutamide** by a factor of 80.

Despite the advantages of targeting multiple domains of the AR, compound **9b** will potentially suffer from poor pharmacokinetic properties due to high MW, HBA, TPSA, and rotatable bond count inferring poor solubility and membrane permeability. Asim and Spring stated that the compounds could have limited membrane permeability as they were less potent than enzalutamide in the luciferase assay, although cLogP and HBD for the compound are within Lipinski's rules. Nevertheless, compound **9b**, is an excellent example of the incorporation of two known AR inhibitors, and its discovery may trigger interest in generating further compounds of this type.

5.3 | NTD targeting analogs identified via high-throughput and virtual screening campaigns

Recent advances in the field of genomics have shortened the time it takes to develop new drugs.¹³¹ However, HTS campaigns remain a powerful means for hit identification, often providing novel structures and future lead

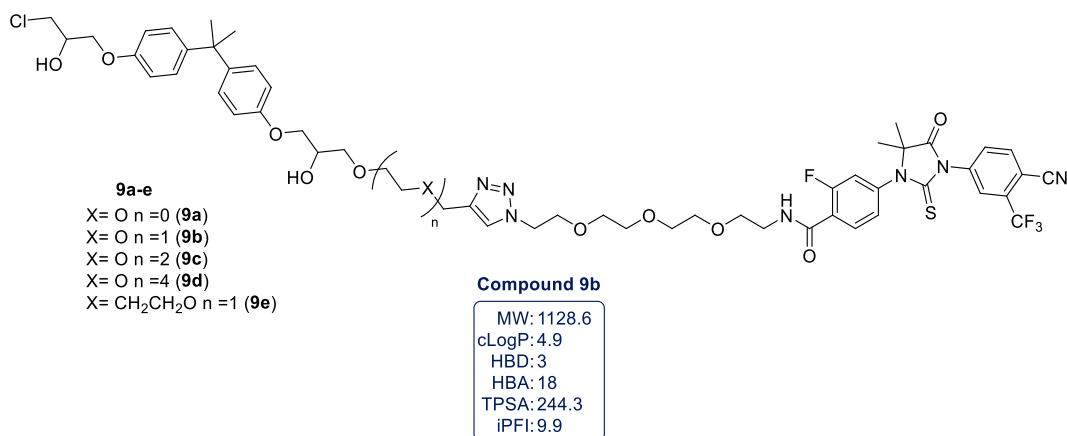


FIGURE 18 Tethered **EPI–enzalutamide** via a linker for targeting the N-terminal domain and ligand-binding domain. cLogP, calculated lipophilicity coefficient; HBA, hydrogen bond acceptor; HBD, hydrogen bond donors; iPFI, intrinsic property forecast index; MW, molecular weight; TPSA, topological polar surface area. [Color figure can be viewed at [wileyonlinelibrary.com](https://onlinelibrary.wiley.com)]

molecules for a wide variety of targets.¹³² HTS is hampered by the need for extensive physical infrastructure and economic resources, but this drawback can be partially addressed through the use of virtual methodologies. Through outsourcing and engaging in collaborations between different bodies, screening campaigns are still a significant part of the armamentarium of pharmaceutical companies and academic groups.

An HTS campaign to identify AR nuclear localization inhibitors identified three hits with IC₅₀ values within 1–5 μ M, one being **IMTPPE**, which was selected for further investigation (Figure 19).¹³³ The compound exhibited an IC₅₀ of 1 μ M in a luciferase assay and inhibited the growth of LNCaP and C4-2 cells (AR-positive) and 22Rv1 cells (AR-V-driven), but not DU145 or PC-3 cells (AR-negative). **IMTPPE** also demonstrated efficacy against enzalutamide-resistant 22Rv1 xenografts.¹³⁴ An SAR study of **IMTPPE**, resulted in the discovery of the **JJ-450** scaffold, with the (–)-enantiomer exhibiting an IC₅₀ value of 1.7 μ M via PSA-luciferase assay.^{135,136} (–)-**JJ-450** has been shown to inhibit the enzalutamide-resistant AR F876L mutant by both luciferase and cell proliferation assays, and slow androgen-mediated nuclear import of the AR. Further efficacy was also demonstrated against both AR-FL and AR-V-driven xenografts. Recently, Cole et al. reported the next-generation analog (+)-**JJ-74-138**, which possessed increased potency in the enzalutamide-resistant LN95 cell line as measured by PSA expression and cell proliferation.¹³⁷

The compounds above were shown to bind directly to the AR and inhibit AR-Vs that lack the LBD, suggesting a mechanism of action independent from this region, however, the specific binding site has not yet been determined. (+)-**JJ-74-138** was shown to inhibit PC-3 cell proliferation, suggesting potential for off-target effects. However, no change in body weight was observed at doses of 10 and 75 mg/kg for (+)-**JJ-74-138** and (–)-**JJ-450**, respectively, reducing concerns over possible toxicity.

In the optimization of **IMTPPE**, the substitution of the thioether for a chiral cyclopropane will likely increase metabolic stability and target specificity; however, the replacement of the isoxazole for a phenyl ring also increased the lipophilicity of (–)-**JJ-450**. The introduction of a pentafluorosulfanyl group, associated with high lipophilicity, exacerbated this increase, resulting in unfavorable cLogP and iPFI values which make (+)-**JJ-74-138** likely to have poor solubility and permeability.¹³⁸

In a previous review of molecules targeting the AR beyond the LBD, Elshan et al. disclosed their own series of analogs that target the NTD, termed JN compounds.²² **JN018** was the initial hit exemplifying the series and elicited a dose-dependent reduction in cell viability in a range of AR-positive prostate cancer cell lines in the 0.1–4 μ M range after 5 days of exposure (Figure 20A).¹³⁹ **JN018** was also shown to inhibit tumor growth in xenograft models

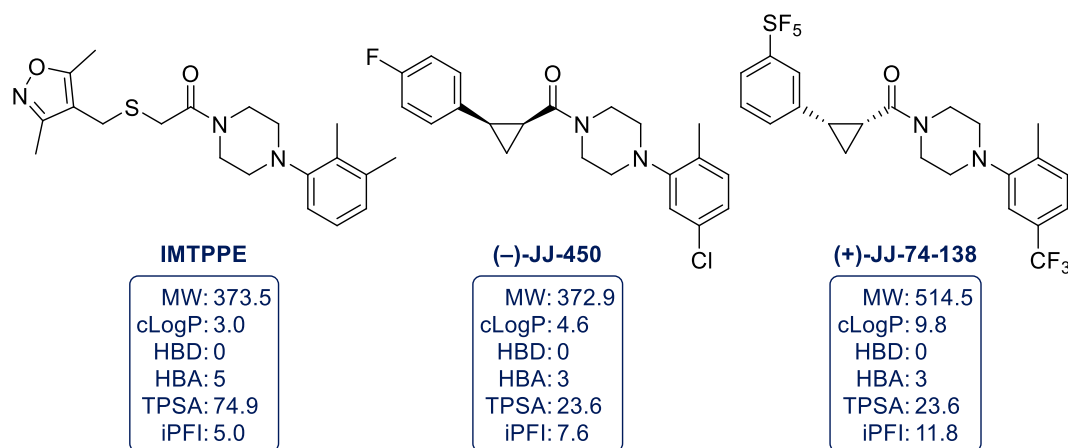


FIGURE 19 Screening hit **IMTPPE** and subsequent derivatized analogs. cLogP, calculated lipophilicity coefficient; HBA, hydrogen bond acceptor; HBD, hydrogen bond donors; iPFI, intrinsic property forecast index; MW, molecular weight; TPSA, topological polar surface area. [Color figure can be viewed at wileyonlinelibrary.com]

with similar efficacy to **enzalutamide**, although signs of toxicity in mice were reported with increased treatment duration.

JN018 exhibits a high cLogP and iPFI, indicative of poor developability.¹⁴⁰ The TPSA of the compound is also particularly low, suggesting it may be able to cross the BBB, leading to the potential for further off-target effects in the CNS.¹⁴¹ In addition, two Michael acceptors are present in **JN018**; although they could potentially be required for the reported covalent mechanism of action, concerns with off-target toxicity via nonspecific reaction with endogenous nucleophiles should be addressed. Moreover, the basic tertiary amine in the molecule, allied with a cLogP of greater than 5, raises concerns regarding hERG inhibition, leading to cardiac side effects.⁶³

In 2017, Ponnusamy et al. reported the selective androgen receptor degrader **UT-155**, which binds to both the NTD and the LBD of the AR (Figure 20B).¹⁴² Degradation of AR-Vs was demonstrated by **UT-155** in vitro, inhibiting transactivation with an IC₅₀ of 78 nM. Substitution of the indole with a fluorinated pyrazole motif afforded

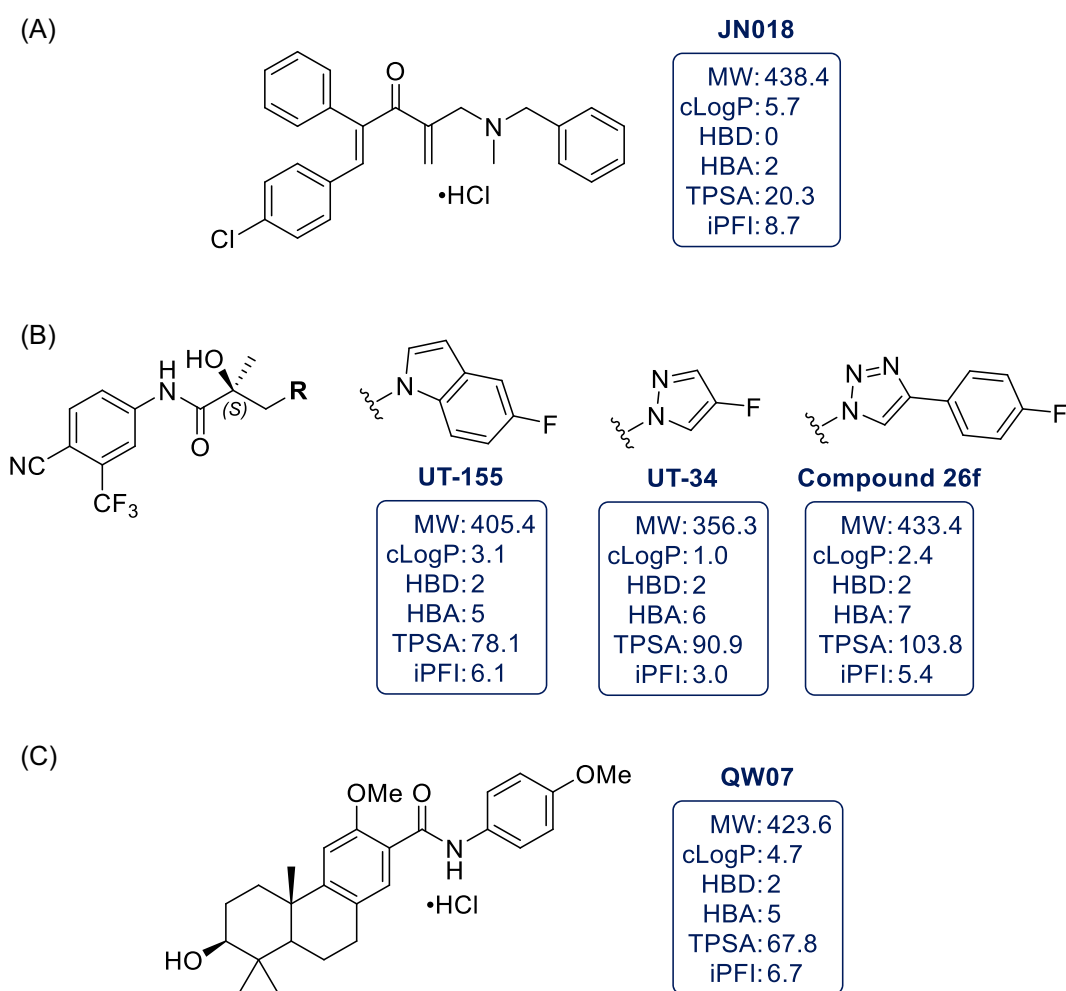


FIGURE 20 (A) Initial hit compound from a splice variant-based screening campaign; (B) Androgen receptor degraders that act via the N-terminal domain (NTD); (C) **QW07**, identified through a screening campaign targeted towards the NTD. cLogP, calculated lipophilicity coefficient; HBA, hydrogen bond acceptor; HBD, hydrogen bond donors; iPFI, intrinsic property forecast index; MW, molecular weight; TPSA, topological polar surface area. [Color figure can be viewed at [wileyonlinelibrary.com](https://onlinelibrary.wiley.com)]

second-generation compound **UT-34**, which demonstrated improved in vivo efficacy, despite a lower in vitro IC_{50} of 200 nM.¹⁴³ This was followed by a further SAR study to improve the pharmacodynamic profile of the series, which yielded compound **26f**.¹⁴⁴

Given that the UT series shares structural features with traditional LBP-antagonists, it is not surprising that **UT-155** displayed an affinity for the LBP; however, mutation of key LBP residues did not decrease anti-AR activity, suggesting that inhibition can be attributed to an alternative mechanism of action which may be consistent with degradation via interaction with the NTD.¹⁴² In addition to this, steady-state fluorescence emission spectroscopy and Biacore surface plasmon resonance studies were utilized to demonstrate the binding of **UT-155** and **UT-34** to the AR-NTD. Considering their developability properties, the UT compounds are an attractive scaffold, with low MW and cLogP values likely contributing to favorable physicochemical properties. The most recent iteration, compound **26f** demonstrates in vivo efficacy against enzalutamide-resistant xenograft models and vastly improved DMPK properties in mouse liver microsomes ($T_{1/2}$ = 265 min) compared to **UT-155** ($T_{1/2}$ = 12 min) and **UT-34** ($T_{1/2}$ = 78 min).¹⁴⁴ The safety profile of **UT-34** has been evaluated, with no off-target effects observed for GPCRs, kinases, other NRs, or inhibition of the hERG ion channel. The favorable DMPK properties and the balanced developability profile of compound **26f** make it a promising lead for addressing treatment resistance in CRPC.

QW07 was identified from a screening campaign via AR-NTD-Gal4DBD-luciferase assay, designed to identify NTD-targeting AR inhibitors (Figure 20C).¹⁴⁵ The compound displayed an IC_{50} value of 5 μ M through a luciferase assay in LNCaP cells and was also validated against multiple AR splice variants. **QW07** represents a novel small molecule that demonstrated greater in vitro efficacy than **EPI-001** and inhibited the expression of four genes that are typically stimulated by the AR (*PSA*, *FKBP5*, *SLC45A3*, and *TMPPRSS2*).

Surface plasmon resonance and biotin antibody assay studies confirmed that the interaction of **QW07** with the AR resides within the NTD.¹⁴⁵ At a dose of 40 mg/kg/day, a significant reduction in tumor size was observed in enzalutamide-resistant xenograft models bearing AR amplification and splice variants; doubling the dose caused no organ damage (judged by histopathological analysis) or detectable changes in body weight. **QW07** was shown not to reduce AR expression or inhibit nuclear translocation and it was proposed that the activity could be attributed to disruption of the interaction between the AR-NTD and CREB-binding protein—a bridging factor that potentially stabilizes the binding of the AR to androgen response elements (AREs).¹⁴⁵ The comparatively high cLogP and iPFI of **QW07** suggest that properties such as solubility or permeability may pose future problems. Having stated this, the encouraging in vivo efficacy data suggest that ADME properties are at least acceptable, although the exact method of administration was not disclosed.

In 2013, Cherkasov et al. discovered **VPC-2055** in a screening campaign for structurally novel AR-LBP antagonists and did not exhibit the same protein degradation mechanism as the other hits identified (Figure 21).¹⁴⁶ Interestingly, **VPC-2055** possesses two chlorohydrin moieties, the same motif responsible for the activity of known NTD inhibitor **EPI-001**. This prompted an SAR exploration that ultimately provided **VPC-220010**, which inhibited AR-V7 with an IC_{50} of 2.7 μ M, fivefold more potent than **EPI-001**.¹⁴⁷ **VPC-220010** also reduced cell viability of LNCaP and AR-V7-dependent 22Rv1 cells more potently than **EPI-001**, whilst having no effect on AR-negative PC-3 cells.

A mechanism of action via the AR-NTD was evidenced by sustained efficacy against an AR-NTD-Gal4-DBD fusion protein in a luciferase assay. Selectivity for the AR over other steroid hormone receptors was also demonstrated using luciferase reporter gene assays. The small and polar nature of **VPC-220010** makes it an attractive compound from a development perspective, with favorable values for MW, cLogP, and iPFI. The presence of multiple reactive groups raises possible concerns regarding off-target toxicity, although the chlorohydrin moiety is present in the well-established EPI scaffold. The microsomal half-life of **VPC-220010** is 30 min, which would likely require optimization in successor compounds. Further development of this molecule may also yield improvements to potency, as in the case of second-generation EPI analogs such as **EPI-7170**.

Work in the Lilly group has taken a different approach to AR inhibition in the form of bispecific antibodies (biAbs).¹⁴⁸ A ligation of two single-chain variable fragments, 3E10—an anti-DNA antibody, and AR441—an anti-AR

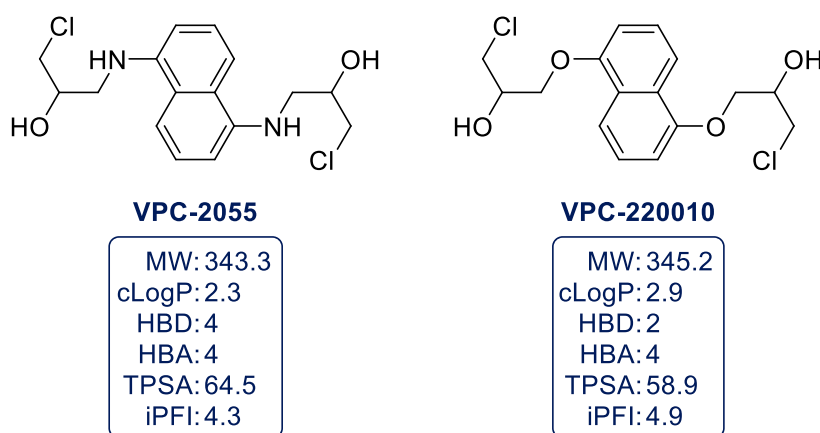


FIGURE 21 N-terminal domain-targeting VPC compounds, **VPC-2055** and **VPC-220010**. cLogP, calculated lipophilicity coefficient; HBA, hydrogen bond acceptor; HBD, hydrogen bond donors; iPFI, intrinsic property forecast index; MW, molecular weight; TPSA, topological polar surface area. [Color figure can be viewed at [wileyonlinelibrary.com](https://onlinelibrary.wiley.com)]

antibody displayed blockage of genomic signaling of both AR-FL and AR-V7 in LNCaP cells. The biAbs successfully met the design rationale of effective cell penetration and target engagement; moreover, the successful inhibition of AR-V7 provided evidence for action via the NTD.

5.4 | Novel liquid–liquid phase separation approach to target the NTD

Very recently, Xie et al. disclosed that the AR forms hormone-dependent nuclear puncta that have properties of liquid-like condensates and are associated with drug resistance.¹⁴⁹ They demonstrated that antiandrogens, **bicalutamide**, and **hydroxyflutamide** blocked puncta formation and transcriptional activity of AR-WT but promoted condensate formation in W742C and T878A. The correlation of liquid–liquid phase separation (LLPS) with AR transcriptional activity postulates that the formation of liquid condensates by antiandrogens with receptor mutants may give rise to drug resistance.¹⁵⁰ Independent isolated regions of the AR were unable to form condensates, but NTD-DBD sequences were able to form puncta similar to the AR-FL. **ET516** was identified through a chemical library screen and inhibited condensate formation and transcriptional activity both in AR-WT and mutant AR bound to the NTD with an IC_{50} value of 0.2 μ M (Figure 22). **ET516** inhibited the growth of cultured prostate cells and xenographs in vivo. Overall, the work by Xie et al. highlights LLPS and AR-NTD as viable drug targets in CRPC.

ET516 possesses a somewhat similar scaffold to the EPI family and resembles **EPI-7170**. **ET516** like **EPI-7170** also exhibits a high MW, above the acceptable limit according to Lipinski's rules and it also possesses a higher cLogP value and inferred iPFI >7. It is likely that these characteristics will lead to low solubility with permeability issues leading to promiscuous off-target effects. **ET516** lacks the hydroxy moiety present in **EPI-7170** which avoids epoxide generation under physiological or basic conditions leading to fewer off-target effects. The introduction of the alkyne as a bioisostere for the ether linker could aid in modulating the pharmacokinetic profile of **ET516**.¹⁵¹ Overall, targeting the novel vulnerability of liquid condensates could help aid the clinical challenge that is CRPC and will be of great interest to see what further compounds will be disclosed (Table 4).

The molecules presented for targeting the NTD span a broad range of physicochemical properties and a number of low MW, and low cLogP hits are amenable to optimization (Figure 23). **EPI-002** is one example that has already undergone extensive investigation to afford the lead compound **EPI-7170**, which possesses good potency,

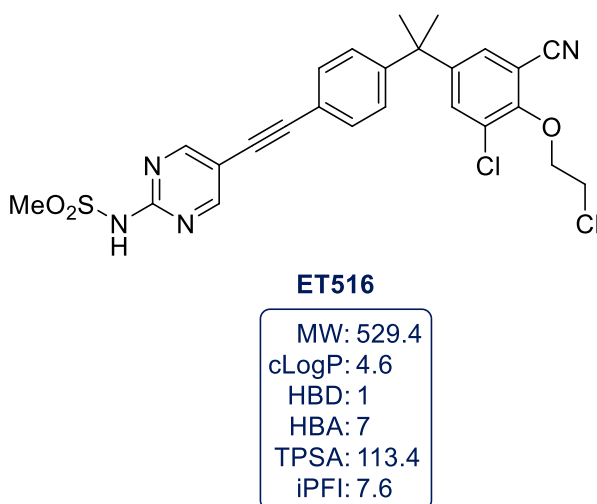


FIGURE 22 Most recent N-terminal domain targeted small molecule, **ET516**, a liquid-liquid phase separation inhibitor. cLogP, calculated lipophilicity coefficient; HBA, hydrogen bond acceptor; HBD, hydrogen bond donors; iPFI, intrinsic property forecast index; MW, molecular weight; TPSA, topological polar surface area. [Color figure can be viewed at wileyonlinelibrary.com]

cLogP, and iPFI, albeit a somewhat high MW. **VPC-220010** took the related chlorohydrin pharmacophore of the EPI series, and applied it to a more compact naphthalene core, concomitantly reducing the MW and cLogP of the scaffold. Further investigation, for example through the replacement of the lipophilic core with heterocyclic derivatives, could modulate the potency and DMPK properties of the series, and a direct comparison with the EPI compounds may clarify the mechanism of action. **UT-34** and **IMTPPE** also emerged as developable hits that have undergone optimization, resulting in compound **26f** which possessed favorable physicochemical properties, and **(+)-JJ-74-138**, for which the cLogP and MW are inflated by the pentafluorosulfonyl group, respectively. **QW07** is a novel scaffold with reasonable potency and MW that presents an opportunity for further examination of its structure-activity and structure-property relationships; a hit-to-lead optimization could tune the efficacy and reduce cLogP, improving this novel chemotype for NTD-directed AR inhibition. Finally, **cinobufagin-3-acetate** presents a new steroidal structure that acts via the NTD and maintains a low cLogP and iPFI. Optimization of this scaffold could center around the requirement of the epoxide moiety to ensure this moiety is not required for the compound's mechanism of action, and seek to reduce the MW.

6 | TARGETING THE DBD

The binding of the DBD to AREs within DNA of androgen-regulated genes is essential for transcriptional activity. The structure of the DBD is highly conserved amongst other NRs, therefore achieving specificity for the AR is a likely challenge for DBD-targeted therapeutics.^{20,97} Recently, advances in computational approaches combined with the disclosure of structural data for the AR-DBD, have enabled the identification of hypothetical sites that are potentially selective for the AR.^{152,153} Approximately 11% of residues in the DBD are subject to a mutation in prostate cancer, highlighting the significance of the DBD in advanced disease.⁹² One possible disadvantage of targeting the DBD rests with the transcription-independent roles of the AR implicated in CRPC and treatment resistance.^{154,155} As the DBD is related solely to the genomic function of AR, molecules that target the region may fail to disrupt any mechanisms whereby CRPC persists unrelated to gene transcription. Nevertheless, the

TABLE 4 Inhibitory activity and assay description of NTD targeting compounds.

Compound	Reported activity AR–IC ₅₀ (μM)	Assay description
Sintokamide A ^{103,104}	10.7	PSA-luciferase assay in LNCaP cells
	35	MTS cell proliferation assay in LNCaP cells
LPY36 ¹⁰⁶	3.5	PSA-luciferase assay in LNCaP cells
	6.9	Alamar blue proliferation assay in LNCaP cells
Dysamide A ¹⁰⁴	10	PSA-luciferase assay in LNCaP cells
Niphatenone B ^{107,108}	5.7	PB-luciferase assay in LNCaP cells
	5.2	PSA-luciferase assay in LNCaP cells
(S)-Mahanine ¹¹¹	N/A	ARR ₃ tk luciferase assay in LNCaP cells (reported graphically only)
Cinobufagin-3-acetate ¹¹³	N/A	Luciferase assay in LNCaP cells (reported graphically only)
EPI-002 ¹¹⁴	7.4	PSA-luciferase assay in LNCaP cells
EPI-7170 ¹²⁰	1.1	PSA-luciferase assay in LNCaP cells
Compound 9b ¹³⁰	1.6	MTT cell viability assay in C4-2b cells
IMTPPE ^{133,134}	1.78	2GFP-AR nuclear localization assay in C4-2 cells
	1	PSA-luciferase assay in C4-2 cells
(-)-JJ-450 ^{135,136}	1.7	PSA-luciferase assay in C4-2 cells
(+)-JJ-74-138 ¹³⁷	1.2/3.0*/4.3 [†]	PSA ELISA assay in C4-2/*LN95/ [†] 22Rv1 cells
JN018 ¹³⁹	0.11	AR inhibition assay
	1.5	Growth inhibition assay
UT-155 ¹⁴²	0.078	GAL4-RE-luciferase assay in HEK-293 cells
UT-34 ¹⁴³	0.20	Dual-luciferase assay in COS7 cells
Compound 26f ¹⁴⁴	0.38	GRE-luciferase assay in HEK-293 cells
QW07 ¹⁴⁵	4.93/7.9*	ARR2-luciferase assay in LNCaP/*22Rv1 cells
	1.9–5.1	Sulforhodamine B cell proliferation assay in LNCaP, 22Rv1, C4-2b, & VCaP cells
VPC-220010 ¹⁴⁷	0.7	eGFP assay in LNCaP cells
	2.7	AR-V7 transcriptional luciferase assay in AR-transfected PC-3 cells
	5.3/10.8*	PrestoBlue cell viability assay in LNCaP/*22Rv1 cells
ET516 ¹⁴⁹	0.2–0.7/5–10	mEGFP assay in LNCaP cells expressing AR (F877L/T878A)/*AR-V7

Abbreviations: AR, androgen receptor; NTD, N-terminal domain.

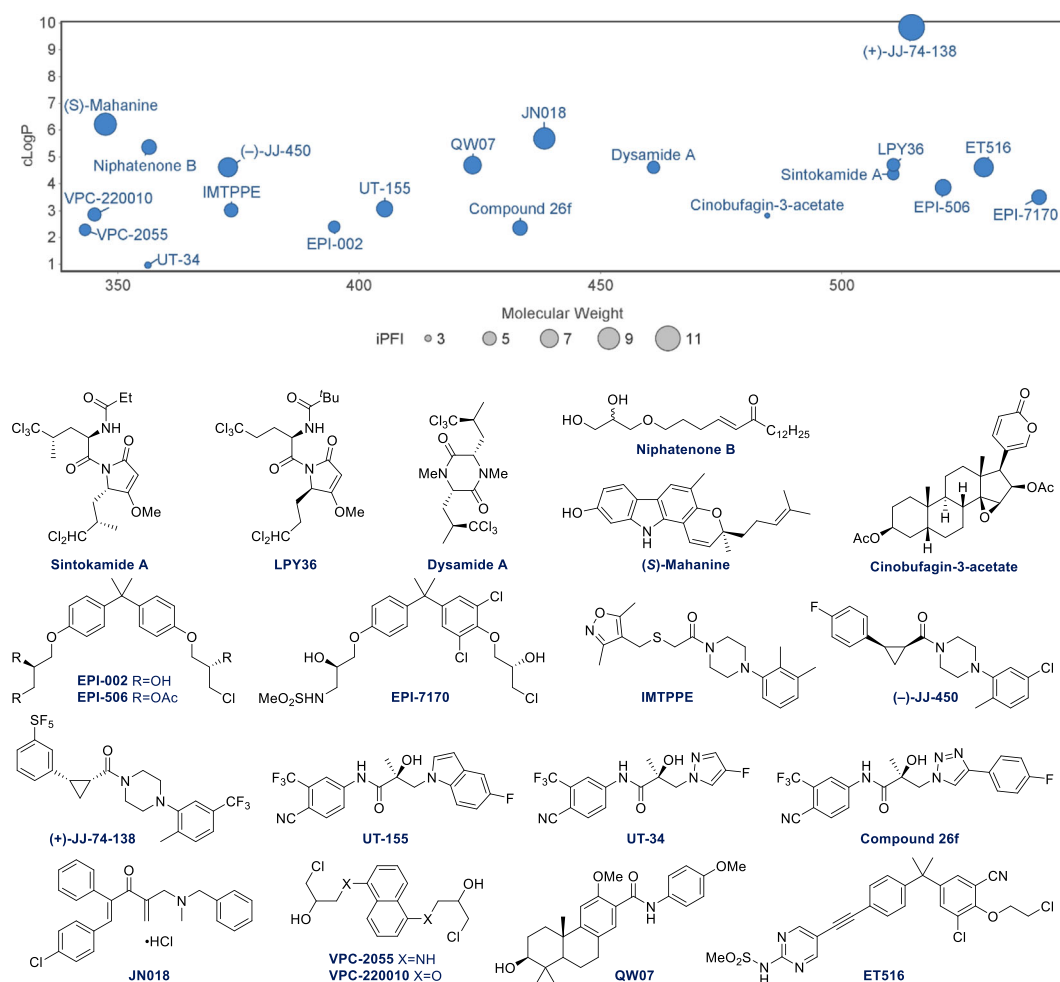


FIGURE 23 Developability overview of compounds that target the N-terminal domain. Compound **9b** was omitted for clarity. [Color figure can be viewed at wileyonlinelibrary.com]

exploration of multiple approaches is likely to be vital for the successful treatment of CRPC. Although reviewed previously, we believe a critical evaluation of the reported structures will afford insight and aid in the future development of drugs for CRPC.^{22,156,157}

6.1 | DBD targeting compounds

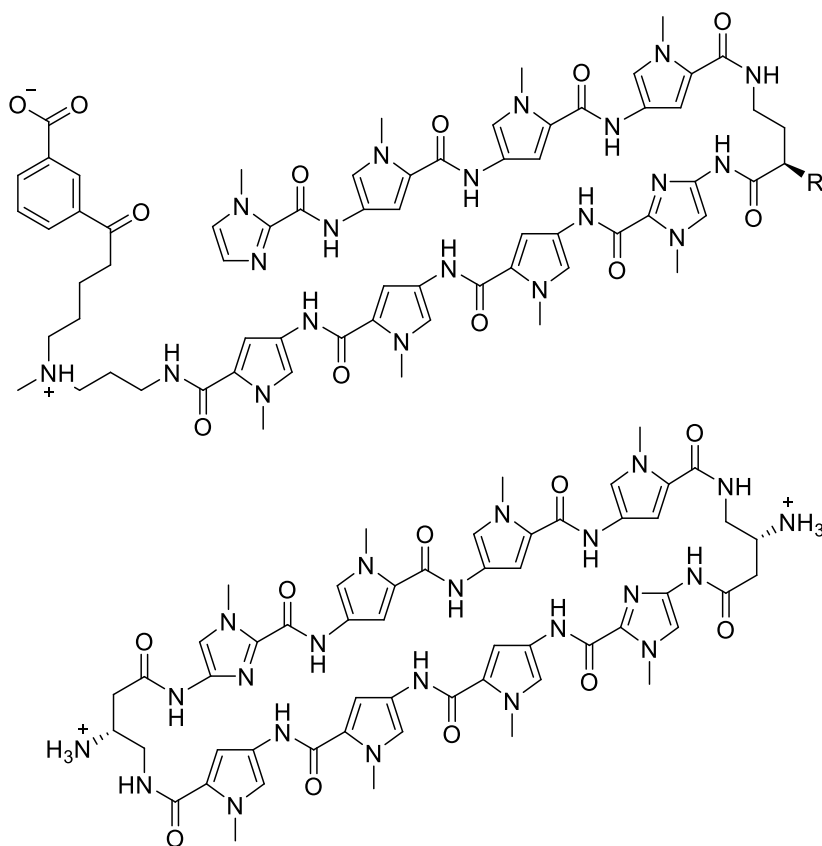
The first reported example of AR inhibition through interaction with DNA takes the form of a sequence-specific, hairpin polyamide minor groove binder, **ARE-1** (Figure 24).¹⁵⁸ The polyamide was reported to bind to AREs within the cognate DNA system resulting in an observed decrease in PSA expression in LNCaP cells with a potency comparable to bicalutamide. **Polyamide 1** was shown to exhibit cytotoxicity against LNCaP and VCaP cell lines with IC₅₀ values of 6.5 and 7.0 μ M, respectively, and demonstrated efficacy in xenograft models.^{159,160} Subsequently, an analogous **cyclic polyamide** was reported to significantly inhibit PSA expression at 3 μ M, whilst demonstrating low hepatic and cardiac toxicity with high microsomal stability, with a half-life greater than 3 h.¹⁶¹ Recently, the

acetylated analog, **ARE-1** was disclosed and displayed a reduction in murine toxicity and improved efficacy in enzalutamide-resistant models, both in vitro and in vivo.^{162–164}

Although these compounds do not directly target the AR protein, the initial reports set an important precedent for direct inhibition of the AR-DNA interface. Since AREs are not identical across the genome, if genes specific to CRPC were to be identified they could potentially be inhibited selectively with tuneable polyamides to minimize off-target effects.¹⁵⁸

The first examples of small molecule inhibition of the AR directly via the DBD were reported in 2009.^{165,166} **Pyrvinium pamoate** and **Harmol hydrochloride** were two hits obtained from a FRET-based conformational assay (Figure 25). Chromatin immunoprecipitation studies identified **Harmol** as blocking DNA occupancy, whereas **Pyrvinium** inhibited the recruitment of RNA pol II to the DNA-bound AR dimer. Luciferase and proliferation assays identified **Pyrvinium** as the lead compound in terms of potency with an IC₅₀ value of 13–24 nM in vitro.

Harmol was excluded from further characterization in vivo due to rapid clearance most likely due to metabolic liabilities, for example, the benzylic position in the pyridine and conjugation of the phenolic alcohol during phase II metabolism. However, **Harmol** possesses a low MW and cLogP, potentially contributing to good solubility and permeability, making the compound a promising structure for future developments which address the metabolic



Polyamide 1 (R = NH₃⁺)

MW: 1357.5
cLogP: -3.6
HBD: 12
HBA: 33
TPSA: 412.0
iPFI: 5.4

ARE-1 (R = NHAc)

MW: 1398.5
cLogP: -1.2
HBD: 11
HBA: 34
TPSA: 413.8
iPFI: 7.8

Cyclic polyamide

MW: 1181.3
cLogP: -9.5
HBD: 12
HBA: 32
TPSA: 411.5
iPFI: -1.5

FIGURE 24 Pyrazole-imidazole scaffolds targeting the DNA-binding domain. cLogP, calculated lipophilicity coefficient; HBA, hydrogen bond acceptor; HBD, hydrogen bond donors; iPFI, intrinsic property forecast index; MW, molecular weight; TPSA, topological polar surface area.

instability. Furthermore, the iPFI value of 5.1 remains in a good range for aqueous solubility, enabling future developments.

The nonspecific toxicity of **Pyrvinium** has been considered, with separate studies demonstrating apoptosis at concentrations of 0.3 and 50 μ M in an MTS assay and Western blot analysis for PARP, respectively.^{167,168} In xenograft models, **Pyrvinium** alone did not display a significant reduction of prostate weight; however, when combined with **bicalutamide**, castration levels of tumor growth suppression were observed.¹⁶⁶ Drug affinity responsive target stability assays and deletion studies have been utilized, which confirm that **Pyrvinium** binds directly to the DBD/hinge of the AR, and has demonstrated activity against homologous hormone receptors such as GR. Pan-receptor activity has been argued both for and against in the area of prostate cancer, possibly avoiding functional replacement of the AR as a driver of CRPC in the case of the former, and being viewed as an undesirable source of off-target effects in the latter.^{167,169} **Pyrvinium** was also shown to be tissue selective and active against a range of AR-Vs in both LNCaP cells and against 22Rv1 in xenograft models.¹⁷⁰ A more recent mechanistic study determined that the activity of **Pyrvinium** is attributed to interactions with residues 609 and 612 in the AR dimer-DNA complex, and proposed that the observed efficacy was due to a conformational change that disrupts PPIs with important cofactors such as RNA pol II, and splicing factors DDX17 and DDX5.¹⁶⁹ Despite these mechanistic studies being specific to the AR, **Pyrvinium** has been implicated in numerous additional signaling pathways, which suggests that the mechanism of any functional activity is likely multidimensional.¹⁷¹ In addition, structural optimization of **Pyrvinium** for enhanced aqueous solubility has been undertaken, resulting in the analog **P24**.¹⁷⁰ The structure of this was not disclosed, therefore it cannot be examined in terms of its optimization campaign and if it addressed issues associated with structural alerts embedded in the compound (e.g., pyridinium species, anilino motif).

Cherkasov et al. undertook the rational design of DBD-targeted therapeutics utilizing the available crystal structure of the AR DBD dimer-DNA complex.^{153,167} Aided by computational modeling, a binding site was proposed to exist in the DBD adjacent to the P-Box region—the region of the DBD that interacts with the DNA major groove.¹⁷² Virtual screening of the ZINC database, followed by an eGFP assay yielded five hit compounds, the most potent of which underwent extensive SAR development, resulting in **VPC-14449** which had an IC₅₀ value of 100 nM determined by eGFP assay (Figure 26A).¹⁶⁷

Binding of **VPC-14449** to the intended DBD region was evidenced using mutagenesis studies, defining the interaction to exist between residues 592 and 594 in the DBD. Moreover, bilayer interferometry was used to

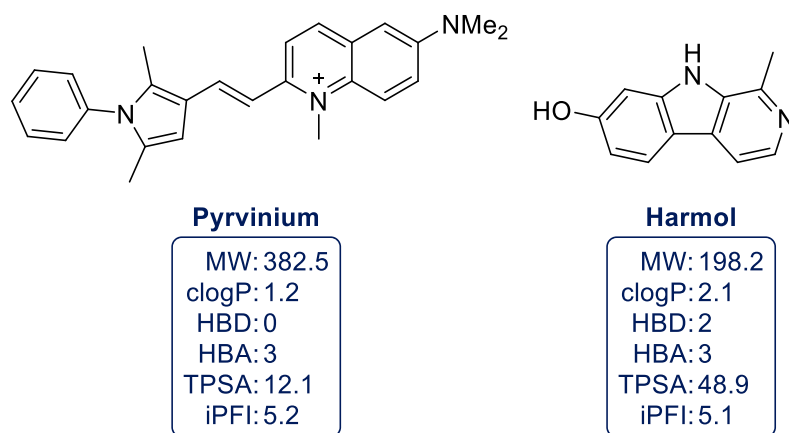


FIGURE 25 Seminal small molecule inhibitors of the AR-DBD. cLogP, calculated lipophilicity coefficient; HBA, hydrogen bond acceptor; HBD, hydrogen bond donors; iPFI, intrinsic property forecast index; MW, molecular weight; TPSA, topological polar surface area. [Color figure can be viewed at wileyonlinelibrary.com]

further substantiate the DBD as the site of action by excluding the possibility of a binding event at the LBP, AF-2, or BF-3 within the LBD, or AREs within target DNA.¹⁶⁷ Despite the conserved nature of nuclear hormone DBD regions, **VPC-14449** displayed negligible inhibition of the ER, GP, and PR. **VPC-14449** was shown to disrupt DBD-chromatin interactions in vitro and inhibit growth of LNCaP cells, enzalutamide-resistant MR49C cells, and AR-V-driven 22Rv1 cells. **VPC-14449** also reduced PSA expression and tumor volume in xenograft models at a dose of 100 mg/kg twice daily, at which no toxicity was observed.^{168,173,174} Notably, optimization of previous hits from the initial screen was also carried out, affording potent DBD-inhibitors **VPC-14332** and **VPC-14452**; however, these assets have only been reported in the patent literature, and therefore are not as extensively characterized as **VPC-14449**.¹⁷⁵ Subsequently, Xu et al. further explored the SAR of **VPC-14449**, but despite extensive analog generation, the potency was not improved.¹⁷⁶

In recent reports from the Cherkasov group, their focus has turned to targeting the D-Box, the region of the DBD involved in homodimerization, which is typically a requirement for DNA binding.^{172,177,178} Using the same virtual screening methodology that they applied to P-Box, four hit compounds were identified and validated.¹⁷⁷ **VPC-17005** was the most potent with an IC₅₀ of 0.7 μ M, and demonstrated activity against enzalutamide-resistant MR49F cells and AR-V-driven 22Rv1 cells, but not AR-negative PC-3 cells, which suggests selectivity for the AR pathway (Figure 26B).

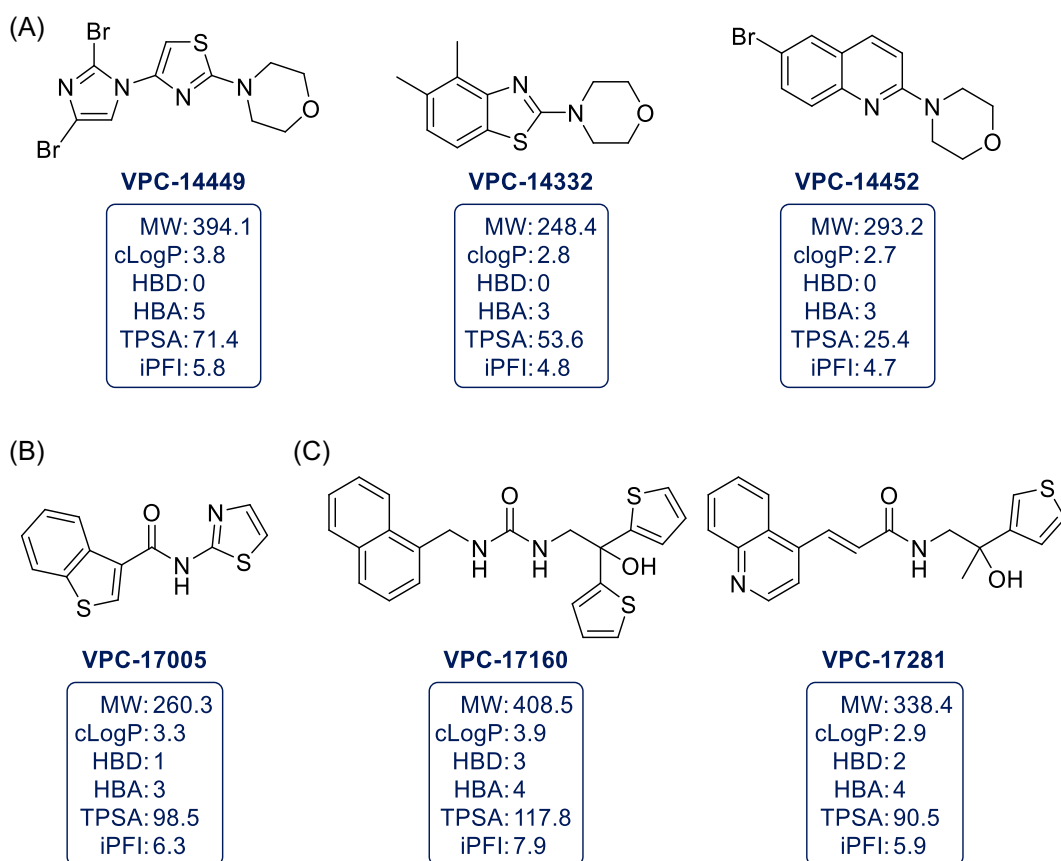


FIGURE 26 (A) First rationally designed AR-DBD targeting inhibitors; (B) inhibitor of AR-DBD dimerization; (C) optimized AR dimerization inhibitors. cLogP, calculated lipophilicity coefficient; HBA, hydrogen bond acceptor; HBD, hydrogen bond donors; iPFI, intrinsic property forecast index; MW, molecular weight; TPSA, topological polar surface area. [Color figure can be viewed at [wileyonlinelibrary.com](https://onlinelibrary.wiley.com)]

Treatment of LNCaP and 22Rv1 cells with **VPC-17005** did not influence the expression of AR protein, which excludes receptor degradation as a possible mechanism of action. In addition, selectivity over other the NRs (ER, GR, and PR) was attributed to the nonconserved residues S597, F606, and S613 by sequence alignment.¹⁷⁷ Mechanistic action via the D-box dimerization interface was demonstrated through the use of a mammalian-two hybrid assay with fused proteins, FRET imaging, BLI experiments, and a lack of inhibition for the dimerization-deficient AR mutant A596T/S597T.

Low MW and moderate cLogP suggest that **VPC-17005** will possess adequate solubility and permeability, although the benzothiophene moiety may present a potential site of metabolic liability. In addition to this, the aminothiazole portion constitutes a known toxicophore which will likely preclude further development.¹⁷⁹ The fragment-like nature of the hit compound, allied with availability of structural data for the AR-DBD enables structure-based optimization of the molecule, for the pursuit of additional receptor–ligand interactions with increased potency.

In subsequent attempts to address the metabolic instability of **VPC-17005**, the authors conducted a further virtual screen of the ZINC database, and utilized a pharmacophore model of **VPC-17005** to identify novel chemotypes with a similar ability to inhibit AR DBD-dimerization.¹⁸⁰ **VPC-17160** and **VPC-17281** were identified and displayed improved antidimerization capacity against AR-V7 compared to **VPC-17005** (Figure 26C). **VPC-17281**, demonstrated marked improvements to microsomal stability and antiproliferative capacity against AR-V7-driven 22Rv1 cells.

From an optimization perspective, **VPC-17281** is likely to be the superior lead compound, due to the comparably favorable physicochemical properties. Furthermore, the microsomal stability is significantly higher, potentially due to the propensity for CYP450-mediated metabolism at 2- and 5-position of the thiophene moiety present.^{80,181} The acrylamide moiety of **VPC-17281** should be considered in future optimization as a possible source of off-target covalent modification, especially given that it is not required for the proposed reversible mechanism of action.

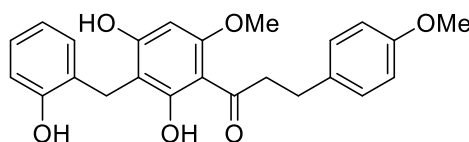
The dihydrochalcone **MF-15** is a synthetic analog of a series of recently reported chalcone natural products, isolated from *Melodorum fruiticosum* (Figure 27A).¹⁸² **MF-15** acts as a dual inhibitor of the AR and AKR1C3, an enzyme involved in intra-tumoral androgen biosynthesis, which is implicated in enzalutamide-resistant CRPC.^{13,183} At a concentration of 10 μ M, **MF-15** inhibited AKR1C3 activity by 87% and significantly inhibited androgen-induced PSA expression. In addition, **MF-15** inhibited AR-FL and AR-V7 in a dose-dependent manner between concentrations of 2.5–10 μ M, and reduced cell viability of enzalutamide resistant 22Rv1 cells in the 0.2–100 μ M range. Kafka et al. proposed that **MF-15** interacts with the P-box in the DBD based on molecular docking studies and nonspecific inhibition for both the AR and GR, which share DBD sequence homology.¹⁸²

MF-15 has acceptable properties in terms of MW and cLogP, leaving opportunities for structural growth and exploration. Replacement of the phenyl rings with heterocycles, or alternative incorporation of polar functionality could modulate activity and favorably influence cLogP. However, it should be noted that the polyphenol functionality is a PAINS structural alert.

Recently, Lee et al. reported a DBD-targeting proteolysis-targeting chimera (PROTAC).¹⁸⁴ **MTX-23** was found to degrade AR-FL, and the clinically relevant splice variants AR-V7 and ARv567, while leaving other steroid hormone receptor levels unaffected (Figure 27B). **MTX-23** also reduced cellular proliferation in AR-positive cell lines, but not AR-negative cell lines. The degradation-based mechanism of **MTX-23** was substantiated through the identification of polyubiquitinated AR-FL and AR-V7 by immunoblot assay. Notably, **MTX-23** also displayed efficacy against LNCaP, VCaP, and 22Rv1 cells that had been cultured to display resistance to the current standard of care CRPC treatments: **abiraterone**, **apalutamide**, **enzalutamide**, and **darolutamide**. In enzalutamide-resistant xenograft models, **MTX-23** significantly reduced tumor size over 5 weeks in combination with **enzalutamide**, compared to enzalutamide treatment alone.

Despite their advantages of higher potency and potential for catalytic protein deterioration, PROTACs often suffer from poor physicochemical properties due to the high MW and a large number of rotatable bonds.¹⁸⁵

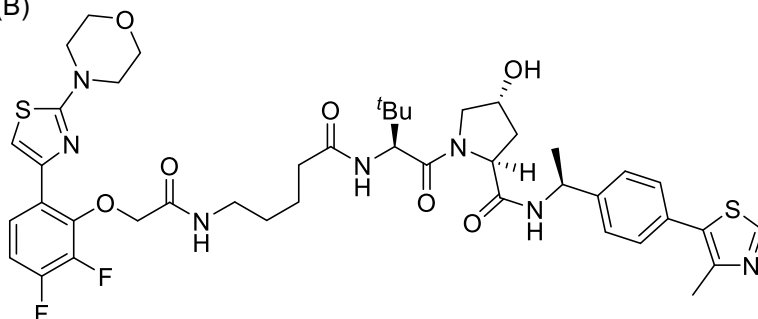
(A)



MF-15

MW: 408.4
cLogP: 4.1
HBD: 3
HBA: 6
TPSA: 96.2
iPFI: 7.1

(B)



MTX-23

MW: 882.1
cLogP: 5.0
HBD: 4
HBA: 14
TPSA: 231.8
iPFI: 9.0

FIGURE 27 (A) Dual inhibitor of the AR-DBD and androgen-synthesizing enzyme AKR1C3; (B) AR-DBD directed PROTAC. cLogP, calculated lipophilicity coefficient; HBA, hydrogen bond acceptor; HBD, hydrogen bond donors; iPFI, intrinsic property forecast index; MW, molecular weight; TPSA, topological polar surface area. [Color figure can be viewed at [wileyonlinelibrary.com](https://onlinelibrary.wiley.com/doi/10.1002/mr.22961)]

MTX-23 exhibits similar characteristics, with large values for MW, cLogP, HBA, and TPSA which increases the likelihood of poor solubility and membrane permeability. Nevertheless, **MTX-23** displayed efficacy in xenograft models when administered both intraperitoneally and orally, suggesting at least moderate bioavailability.

In general, the molecules that target the DBD all comply with Lipinski's rules, with the exception of **MTX-23** (Figure 28). Despite rapid clearance, **Harmol** possesses good potency and fragment-like properties, making it an attractive starting point to optimize inhibition of DNA occupancy.¹⁸⁶ **Pyrvinium** also resides in druglike chemical space and displays potent AR inhibition in a luciferase assay, optimization has already been carried out and we await the disclosure of next-generation analog, **P24**.¹⁷⁰ The P-box-targeting VPC compounds all have druglike properties in terms of MW, cLogP, HBD/A, TPSA, and iPFI, making oral absorption likely. They have also undergone extensive SAR exploration, particularly **VPC-14449**, and represent the most thoroughly validated class of AR-DBD inhibitors to date. The lead D-box-targeting compound, **VPC-17281** also presents with good physicochemical properties for solubility and permeability, and a balance of polar and lipophilic groups (Table 5).

7 | TARGETING THE HINGE REGION

The HR is a short flexible linker between the DBD and the LBD that contains one half of a bipartite nuclear localization signal.¹⁸⁷ Mutation and deletion studies have demonstrated that the HR, particularly residues 628 to 646, exerts inhibitory regulation over ligand-dependant AF-2 function, modulates transcriptional activity and is implicated in constitutively active double mutants.^{188–190} It also plays a role in DNA binding, nuclear translocation, transactivation and C–N interaction of the AR.^{191–194} While the role of the HR is more than a passive linker, it has received scant attention and is widely overlooked in the context of targeting the AR in the treatment of CRPC.

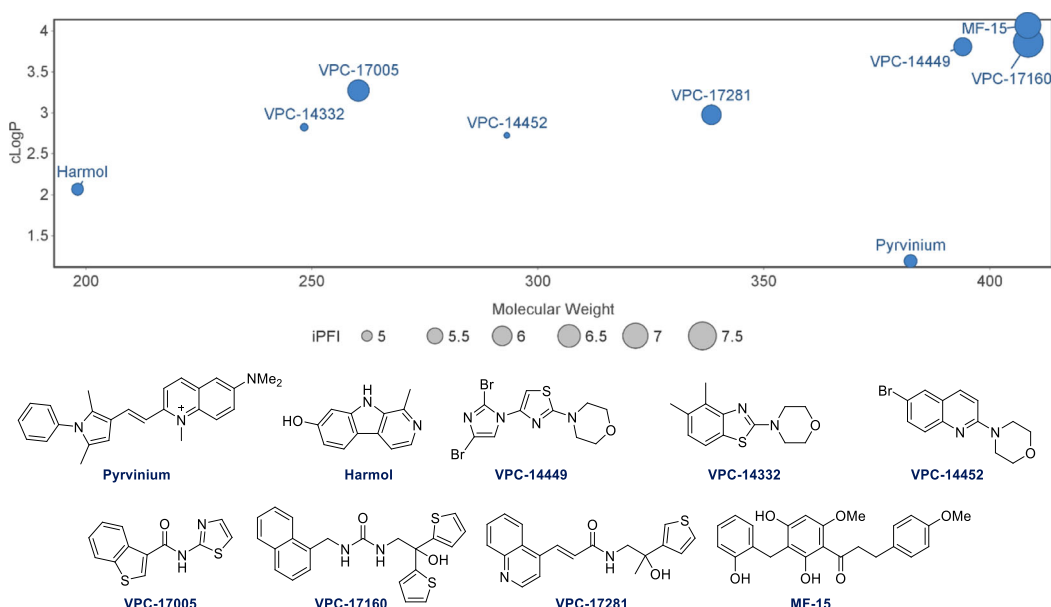


FIGURE 28 Developability overview of compounds that target the DNA-binding domain. [Color figure can be viewed at wileyonlinelibrary.com]

Despite the implication of the HR in numerous functional processes, no small molecule inhibitors of AR that directly target the HR have been reported to date. In terms of chemologics, **EZN-4176** is an antisense oligonucleotide that targets the HR of AR mRNA with some efficacy, although technically lies outside the principal focus of this review as it does not target the AR protein.^{195,196} There are also examples of AR inhibition via the interruption of posttranslational modifications that occur at the HR, but are known to target other proteins such as histone acetyltransferases, rather than engaging in direct interaction with the AR itself.¹⁹⁷ Further mechanistic investigation of the HR and its roles could afford valuable insight and lead to possible therapeutic targets for CRPC.

8 | MISCELLANEOUS COMPOUNDS

In addition to the above, **ASC-J9** (dimethylcurcumin) is a small molecule enhancer of AR degradation (Figure 29A).^{198,199} Mechanistically, it is reported to function via selectively interrupting interactions between the AR and its coregulators, ultimately resulting in reduced transcriptional activity and enhancing proteasomal degradation. **ASC-J9** has been shown to inhibit growth of androgen-sensitive and castration resistant cell lines and suppresses tumor growth in xenograft models. Addressing the lipophilic nature of **ASC-J9** and removing the central Michael acceptor moieties, despite their presence in the natural curcuminoid scaffold, may serve as potential focus points during future optimization.

Finally, **AZD3514** is a small molecule inhibitor of the AR, which has a bimodal mechanism of action, acting both via disruption of androgen-promoted nuclear translocation, and downregulation of receptor levels (Figure 29B).²⁰⁰ Two phase 1 clinical trials (NCT01351688, NCT01162395) assessing **AZD3514** have taken place, wherein moderate efficacy was demonstrated, albeit accompanied by an unacceptable side effect profile. Although the MW of **AZD3514** is above 500, the remaining metrics such as cLogP, iPFI, and TPSA are acceptable; combined with demonstrable efficacy, this encourages further investigation of this chemotype.

TABLE 5 Inhibitory activity and assay description of DBD targeting compounds.

Compound	Reported activity AR–IC ₅₀ (μM)	Assay description
Polyamide 1 ^{159,160}	6.5/7.0*	WST-1 cell viability assay in LNCaP/*VCaP cells
ARE-1 ¹⁵⁸	6.2	WST-1 cell viability assay in LNCaP cells
Cyclic polyamide ¹⁶¹	N/A	PSA mRNA expression in LNCaP cells (reported graphically only)
Pyrvinium ^{165,166}	0.012/0.024*	PSA-luciferase assay in LAPC4/*LNCaP cells
Harmol ^{165,166}	0.11/0.13*	PSA-luciferase assay in LAPC4/*LNCaP cells
VPC-14449 ^{153,167,172}	0.10	eGFP assay in LNCaP cells
	0.17	PSA expression assay in LNCaP cells
	0.34	ARR ₃ tk PB-luciferase in PC-3 cells
	15.2/0.57*	PrestoBlue cell viability assay in 22Rv1 (AR-V7-driven)/*MR49F (F876L driven) cells
VPC-14332 ¹⁷⁵	0.068	eGFP assay in LNCaP cells
	0.058	PSA expression assay in LNCaP cells
VPC-14452 ¹⁷⁵	0.11	eGFP assay in LNCaP cells
	0.058	PSA expression assay in LNCaP cells
VPC-17005 ¹⁷⁷	0.73	eGFP assay in LNCaP cells
	0.69	PSA expression assay in LNCaP cells
	1.46/20.8*/1.8 [†]	PrestoBlue cell viability assay in LNCaP/*22Rv1 (AR-V7-driven)/*MR49F (F876L driven) cells
	10	AR-V7 ARR ₃ tk-nanoLuciferase reporter
VPC-17160 ¹⁸⁰	2	eGFP assay in LNCaP cells
	2	PSA expression assay in LNCaP cells
	6	AR-V7 ARR ₃ tk-nanoLuciferase reporter
VPC-17281 ¹⁸⁰	5	eGFP assay in LNCaP cells
	6	PSA expression assay in LNCaP cells
	6	AR-V7 ARR ₃ tk-nanoLuciferase reporter
	25/10*	PrestoBlue cell viability assay in LNCaP/*22Rv1 cells
MF-15 ¹⁸²	N/A	PSA/FKBP5 expression in 22Rv1 cells (reported graphically only)
MTX-23 ¹⁸⁴	2/0.37*	Immunoblot degradation assay for AR-FL/*AR-V7 protein

Abbreviations: AR, androgen receptor; DBD, DNA-binding domain.

9 | CONCLUSIONS

Many of the compounds presented in this review combine good developability profiles with promising efficacy against the AR in a range of assays that demonstrate novel modes of action (Figure 30). Those assets with reasonable lipophilicity and low MWs are more likely to be developed into advanced leads, or ultimately clinical candidates; not only because there are further opportunities for structural growth and exploration but also because they avoid the majority of the potential liabilities present in suboptimal molecules, that is, off-target effects, low

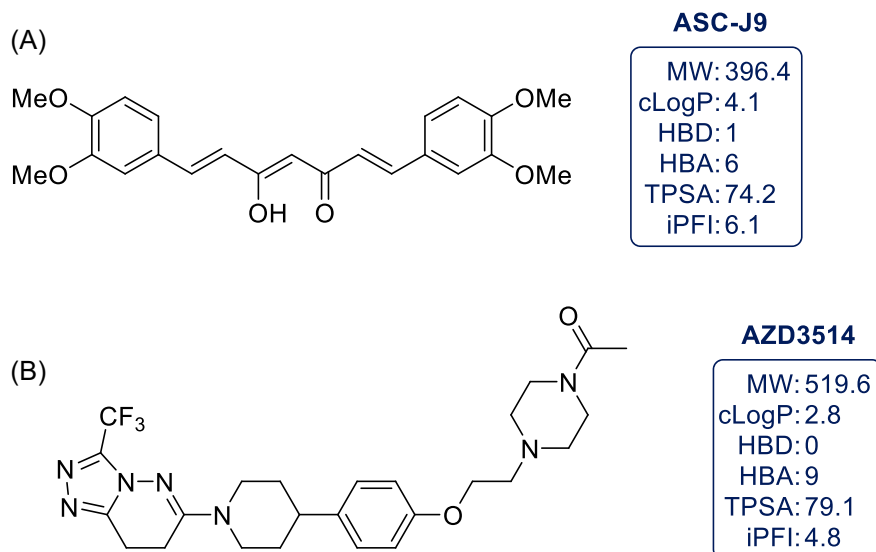


FIGURE 29 (A) AR degradation enhancer ASC-J9; (B) dual mechanism AR inhibitor AZD3514. cLogP, calculated lipophilicity coefficient; HBA, hydrogen bond acceptor; HBD, hydrogen bond donors; iPFI, intrinsic property forecast index; MW, molecular weight; TPSA, topological polar surface area. [Color figure can be viewed at wileyonlinelibrary.com]

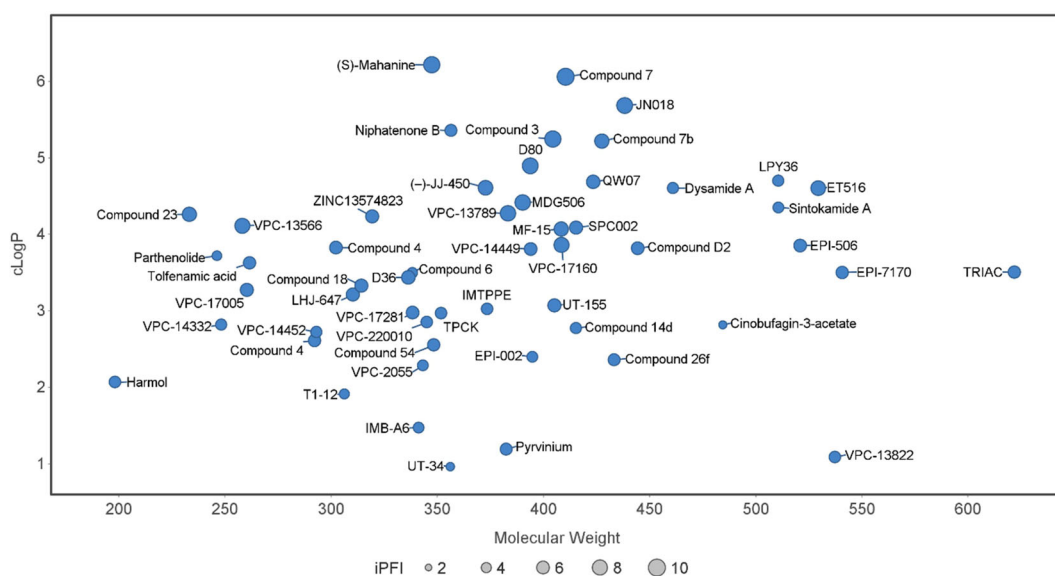


FIGURE 30 Developability overview of all compounds considered within this review. MTX-23, (+)-JJ-74-138, and compound **9b** were omitted for clarity. [Color figure can be viewed at wileyonlinelibrary.com]

solubility, poor permeability, and presence of metabolic hotspots.⁶⁹ Through careful control of the developability properties of candidate molecules in early-stage drug development, researchers can ensure that time and resources are focused on higher-quality compounds to minimize drug attrition rates throughout the discovery pipeline.²⁰¹ Many of the current approaches are well-balanced in this regard and are likely to be explored in future publications.

It remains to be seen whether the development of more efficient and mechanistically diverse inhibitors of the AR will overcome treatment resistance in the clinical setting. The success seen with second-generation antiandrogens, coupled with the fact that the AR gene is the most commonly upregulated gene in CRPC patients, warrants additional future development of AR-based CRPC therapies that do not target the canonical LBD.^{202,203}

DATA AVAILABILITY STATEMENT

Data relating to calculated molecular properties of molecules reported in the review is available from the corresponding authors on request.

ORCID

Martyn C. Henry  <http://orcid.org/0000-0002-1681-7491>

REFERENCES

- World Health Organisation. Global Cancer Observatory. 2020. https://gco.iarc.fr/today/online-analysis-table?v=2018&mode=cancer&mode_population=continents&population=900&populations=900&key=asr&sex=1&cancer=39&type=0&statistic=5&prevalence=0&population_group=0&ages_group%5B%5D=0&ages_group%5B%5D=17&nb_items=5&group
- Siegel RL, Miller KD, Jemal A. Cancer statistics, 2019. *CA Cancer J Clin*. 2019;69:7-34.
- Figg WD, Chau CH, Small EJ. Drug Management of Prostate Cancer. 2010.
- Harris WP, Mostaghel EA, Nelson PS, Montgomery B. Androgen deprivation therapy: progress in understanding mechanisms of resistance and optimizing androgen depletion. *Nat Clin Pract Urol*. 2009;6:76-85.
- Novara G, Galfano A, Secco S, Ficarra V, Artibani W. Impact of surgical and medical castration on serum testosterone level in prostate cancer patients. *Urol Int*. 2009;82:249-255.
- Huggins C. Studies on prostatic cancer: II. The effects of castration on advanced carcinoma of the prostate gland. *AArch Surg*. 1941;43:209-223.
- Pienta KJ, Bradley D. Mechanisms underlying the development of androgen-independent prostate cancer. *Clin Cancer Res*. 2006;12:1665-1671.
- Kirby M, Hirst C, Crawford ED. Characterising the castration-resistant prostate cancer population: a systematic review: the epidemiology of CRPC. *Int J Clin Pract*. 2011;65:1180-1192.
- Reid J, Kelly SM, Watt K, Price NC, McEwan IJ. Conformational analysis of the androgen receptor amino-terminal domain involved in transactivation. *J Biol Chem*. 2002;277:20079-20086.
- Modi PK, Faiena I, Kim IY. Chapter 3 - Androgen receptor. In: Mydlo JH, Godec CJ, eds. *Prostate Cancer*. 2nd ed. Academic Press; 2016:21-28.
- Yap TA, Smith AD, Ferraldeschi R, Al-Lazikani B, Workman P, De Bono JS. Drug discovery in advanced prostate cancer: translating biology into therapy. *Nat Rev Drug Discovery*. 2016;15:699-718.
- Chen CD, Welsbie DS, Tran C, et al. Molecular determinants of resistance to antiandrogen therapy. *Nature Med*. 2004;10:33-39.
- Stanbrough M, Bubley GJ, Ross K, et al. Increased expression of genes converting adrenal androgens to testosterone in androgen-independent prostate cancer. *Cancer Res*. 2006;66:2815-2825.
- Helsen C, Van den Broeck T, Voet A, et al. Androgen receptor antagonists for prostate cancer therapy. *Endocr Relat Cancer*. 2014;21:T105-T118.
- Rice MW, Pandya JD, Shear DA. Gut microbiota as a therapeutic target to ameliorate the biochemical, neuroanatomical, and behavioral effects of traumatic brain injuries. *Front Neurol*. 2019;10:875.
- Crawford ED, Schellhammer PF, McLeod DG, et al. Androgen receptor targeted treatments of prostate cancer: 35 years of progress with antiandrogens. *J Urol*. 2018;200:956-966.
- Chandrasekar T, Yang JC, Gao AC, Evans CP. Mechanisms of resistance in castration-resistant prostate cancer (CRPC). *Transl Androl Urol*. 2015;4:365-380.
- Schmidt KT, Huitema ADR, Chau CH, Figg WD. Resistance to second-generation androgen receptor antagonists in prostate cancer. *Nat Rev Urol*. 2021;18:209-226.
- Crona D, Whang Y. Androgen receptor-dependent and -independent mechanisms involved in prostate cancer therapy resistance. *Cancers*. 2017;9:67.
- Monaghan A, McEwan I. A sting in the tail: the n-terminal domain of the androgen receptor as a drug target. *Asian J Androl*. 2016;18:687-694.
- Rettig M, Jung ME, Elshan NGRD, An J. Inhibitors of the n-terminal domain of the androgen receptor. 2018.

22. Elshan NGRD, Rettig MB, Jung ME. Molecules targeting the androgen receptor (AR) signaling axis beyond the AR ligand-binding domain. *Med Res Rev.* 2019;39:910-960.
23. Cato L, de Tribolet-Hardy J, Lee I, et al. ARv7 represses tumor-suppressor genes in castration-resistant prostate cancer. *Cancer Cell.* 2019;35:401-413.e6.
24. Sander T, Freyss J, von Korff M, Rufener C. DataWarrior: an open-source program for chemistry aware data visualization and analysis. *J Chem Inf Model.* 2015;55:460-473.
25. Lipinski CA, Lombardo F, Dominy BW, Feeney PJ. Experimental and computational approaches to estimate solubility and permeability in drug discovery and development settings. *Adv Drug Deliv Rev.* 1997;23:3-25.
26. Young RJ, Green DVS, Luscombe CN, Hill AP. Getting physical in drug discovery II: the impact of chromatographic hydrophobicity measurements and aromaticity. *Drug Discovery Today.* 2011;16:822-830.
27. Balani S, Miwa G, Gan L-S, Wu J-T, Lee F. Strategy of utilizing in vitro and in vivo ADME tools for lead optimization and drug candidate selection. *Curr Top Med Chem.* 2005;5:1033-1038.
28. van Breemen RB, Li Y. Caco-2 cell permeability assays to measure drug absorption. *Expert Opin Drug Metab Toxicol.* 2005;1:175-185.
29. Abbasi A. Darolutamide as a Second-Generation androgen receptor inhibitor in the treatment of prostate cancer. *Curr Mol Med.* 2021;21:332-346.
30. Veber DF, Johnson SR, Cheng H-Y, Smith BR, Ward KW, Kopple KD. Molecular properties that influence the oral bioavailability of drug candidates. *J Med Chem.* 2002;45:2615-2623.
31. Moilanen AM, Riikonen R, Oksala R, et al. Discovery of ODM-201, a new-generation androgen receptor inhibitor targeting resistance mechanisms to androgen signaling-directed prostate cancer therapies. *Sci Rep.* 2015;5:12007.
32. Zhao J, Ning S, Lou W, et al. Cross-Resistance among Next-Generation antiandrogen drugs through the AKR1C3/AR-V7 axis in advanced prostate cancer. *Mol Cancer Ther.* 2020;19:1708-1718.
33. Huang Y, Jiang X, Liang X, Jiang G. Molecular and cellular mechanisms of castration resistant prostate cancer. *Oncol Lett.* 2018;15:6063-6076.
34. Watson PA, Arora VK, Sawyers CL. Emerging mechanisms of resistance to androgen receptor inhibitors in prostate cancer. *Nat Rev Cancer.* 2015;15:701-711.
35. Steinkamp MP, O'Mahony OA, Brogley M, et al. Treatment-dependent androgen receptor mutations in prostate cancer exploit multiple mechanisms to evade therapy. *Cancer Res.* 2009;69:4434-4442.
36. Korpala M, Korn JM, Gao X, et al. An F876L mutation in androgen receptor confers genetic and phenotypic resistance to MDV3100 (enzalutamide). *Cancer Discov.* 2013;3:1030-1043.
37. Li Y, Chan SC, Brand LJ, Hwang TH, Silverstein KAT, Dehm SM. Androgen receptor splice variants mediate enzalutamide resistance in castration-resistant prostate cancer cell lines. *Cancer Res.* 2013;73:483-489.
38. Langley E, Kemppainen JA, Wilson EM. Intermolecular NH₂-carboxyl-terminal interactions in androgen receptor dimerization revealed by mutations that cause androgen insensitivity. *J Biol Chem.* 1998;273:92-101.
39. He B, Kemppainen JA, Voegel JJ, Gronemeyer H, Wilson EM. Activation function 2 in the human androgen receptor ligand binding domain mediates interdomain communication with the NH₂-terminal domain. *J Biol Chem.* 1999;274:37219-37225.
40. He B, Kemppainen JA, Wilson EM. FXXLF and WXXLF sequences mediate the NH₂-terminal interaction with the ligand binding domain of the androgen receptor. *J Biol Chem.* 2000;275:22986-22994.
41. Feng W, Ribeiro RCJ, Wagner RL, et al. Hormone-dependent coactivator binding to a hydrophobic cleft on nuclear receptors. *Science.* 1979;199(280):1747-1749.
42. He B, Lee LW, Mingos JT, Wilson EM. Dependence of selective gene activation on the androgen receptor NH₂- and COOH-terminal interaction. *J Biol Chem.* 2002;277:25631-25639.
43. Chang C, Abdo J, Hartney T, McDonnell DP. Development of peptide antagonists for the androgen receptor using combinatorial peptide phage display. *Mol Endocrinol.* 2005;19:2478-2490.
44. Hsu CL, Liu JS, Wu PL, et al. Identification of a new androgen receptor (AR) co-regulator BUD31 and related peptides to suppress wild-type and mutated AR-mediated prostate cancer growth via peptide screening and X-ray structure analysis. *Mol Oncol.* 2014;8:1575-1587.
45. van de Wijngaert DJ, Dubbink HJ, Molier M, de Vos C, Jenster G, Trapman J. Inhibition of androgen receptor functions by gelsolin FxxFF peptide delivered by transfection, cell-penetrating peptides, and lentiviral infection. *Prostate.* 2011;71:241-253.
46. Gunther JR, Parent AA, Katzenellenbogen JA. Alternative inhibition of androgen receptor signaling: peptidomimetic pyrimidines as direct androgen receptor/coactivator disruptors. *ACS Chem Biol.* 2009;4:435-440.
47. Leeson PD, Springthorpe B. The influence of drug-like concepts on decision-making in medicinal chemistry. *Nat Rev Drug Discovery.* 2007;6(11):881-890.
48. Sterling T, Irwin JJ. ZINC 15—ligand discovery for everyone. *J Chem Inf Model.* 2015;55:2324-2337.

49. Axerio-Cilies P, Lack NA, Nayana MRS, et al. Inhibitors of androgen receptor activation function-2 (AF2) site identified through virtual screening. *J Med Chem*. 2011;54:6197-6205.
50. Caboni L, Kinsella GK, Blanco F, et al. "True" antiandrogens—selective non-ligand-binding pocket disruptors of androgen receptor–coactivator interactions: novel tools for prostate cancer. *J Med Chem*. 2012;55:1635-1644.
51. Caboni L, Gálvez-Llompert M, Gálvez J, et al. Molecular topology applied to the discovery of 1-Benzyl-2-(3-fluorophenyl)-4-hydroxy-3-(3-phenylpropanoyl)-2H-pyrrole-5-one as a non-ligand-binding-pocket antiandrogen. *J Chem Inf Model*. 2014;54:2953-2966.
52. SPECS. SPECS Database. 2020. www.specs.net
53. Weiser PT, Williams AB, Chang CY, McDonnell DP, Hanson RN. 3,3'-Disubstituted bipolar biphenyls as inhibitors of nuclear receptor coactivator binding. *Bioorg Med Chem Lett*. 2012;22:6587-6590.
54. Ravindranathan P, Lee TK, Yang L, et al. Peptidomimetic targeting of critical androgen receptor–coregulator interactions in prostate cancer. *Nat Commun*. 2013;4:1923.
55. Lee TK, Ravindranathan P, Sonavane R, Raj GV, Ahn JM. A structure–activity relationship study of Bis-Benzamides as inhibitors of androgen receptor–coactivator interaction. *Molecules*. 2019;24:2783.
56. Hua Y, Shun TY, Strock CJ, Johnston PA. High-content positional biosensor screening assay for compounds to prevent or disrupt androgen receptor and transcriptional intermediary factor 2 protein–protein interactions. *Assay Drug Dev Technol*. 2014;12:395-418.
57. Hsu CL, Liu JS, Lin TW, et al. Characterization of a novel androgen receptor (AR) coregulator RIPK1 and related chemicals that suppress AR-mediated prostate cancer growth via peptide and chemical screening. *Oncotarget*. 2017;8:69508-69519.
58. Liu Y, Wu M, Wang T, et al. Structural based screening of antiandrogen targeting activation function-2 binding site. *Front Pharmacol*. 2018;9:01419.
59. Chai X, Sun H, Zhou W, et al. Discovery of N-(4-(Benzyloxy)-phenyl)-sulfonamide derivatives as novel antagonists of the human androgen receptor targeting the activation function 2. *J Med Chem*. 2022;65:2507-2521.
60. Peredy TR. *Encyclopedia of Toxicology*. Elsevier; 2014.
61. Blanco F, Egan B, Caboni L, et al. Study of E/Z isomerization in a series of novel non-ligand binding pocket androgen receptor antagonists. *J Chem Inf Model*. 2012;52:2387-2397.
62. Weiser PT, Chang CY, McDonnell DP, Hanson RN. 4,4'-Unsymmetrically substituted 3,3'-biphenyl alpha helical proteomimetics as potential coactivator binding inhibitors. *Bioorg Med Chem*. 2014;22:917-926.
63. Jamieson C, Moir EM, Rankovic Z, Wishart G. Medicinal chemistry of hERG optimizations: highlights and hang-ups. *J Med Chem*. 2006;49:5029-5046.
64. Nepali K, Lee HY, Liou JP. Nitro-group-containing drugs. *J Med Chem*. 2019;62:2851-2893.
65. Patel M, Kranz M, Munoz-Muriedas J, et al. A pharma-wide approach to address the genotoxicity prediction of primary aromatic amines. *Comput Toxicol*. 2018;7:27-35.
66. Fancher AT, Hua Y, Camarco DP, Close DA, Strock CJ, Johnston PA. Reconfiguring the AR-TIF2 protein–protein interaction HCS assay in prostate cancer cells and characterizing the hits from a LOPAC screen. *Assay Drug Dev Technol*. 2016;14:453-477.
67. Fancher AT, Hua Y, Camarco DP, Close DA, Strock CJ, Johnston PA. High-content screening campaign to identify compounds that inhibit or disrupt androgen receptor–transcriptional intermediary factor 2 protein–protein interactions for the treatment of prostate cancer. *Assay Drug Dev Technol*. 2018;16:297-319.
68. Fancher AT, Hua Y, Strock CJ, Johnston PA. Assays to interrogate the ability of compounds to inhibit the AF-2 or AF-1 transactivation domains of the androgen receptor. *Assay Drug Dev Technol*. 2019;17:364-386.
69. Hann MM. Molecular obesity, potency and other addictions in drug discovery. *MedChemComm*. 2011;2:349-355.
70. Boike L, Henning NJ, Nomura DK. Advances in covalent drug discovery. *Nat Rev Drug Discovery*. 2022;21:881-898.
71. Estébanez-Perpiñá E, Arnold LA, Nguyen P, et al. A surface on the androgen receptor that allosterically regulates coactivator binding. *Proc Natl Acad Sci U S A*. 2007;104:16074-16079.
72. Joseph JD, Wittmann BM, Dwyer MA, et al. Inhibition of prostate cancer cell growth by second-site androgen receptor antagonists. *Proc Natl Acad Sci U S A*. 2009;106:12178-12183.
73. Lack NA, Axerio-Cilies P, Tavassoli P, et al. Targeting the binding function 3 (BF3) site of the human androgen receptor through virtual screening. *J Med Chem*. 2011;54:8563-8573.
74. Munuganti RSN, Leblanc E, Axerio-Cilies P, et al. Targeting the binding function 3 (BF3) site of the androgen receptor through virtual screening. 2. Development of 2-((2-phenoxyethyl) thio)-1H-benzimidazole derivatives. *J Med Chem*. 2013;56:1136-1148.
75. Munuganti RSN, Hassona MDH, Leblanc E, et al. Identification of a potent antiandrogen that targets the BF3 site of the androgen receptor and inhibits enzalutamide-resistant prostate cancer. *Chem Biol*. 2014;21:1476-1485.
76. Dalal K, Morin H, Ban F, et al. Small molecule-induced degradation of the full length and V7 truncated variant forms of human androgen receptor. *Eur J Med Chem*. 2018;157:1164-1173.

77. Lallous N, Leblanc E, Munuganti RSN, et al. Targeting binding function-3 of the androgen receptor blocks its co-chaperone interactions, nuclear translocation, and activation. *Mol Cancer Ther*. 2016;15:2936-2945.
78. Leblanc E, Ban F, Cavga AD, et al. Development of 2-(5,6,7-trifluoro-1H-Indol-3-yl)-quinoline-5-carboxamide as a potent, selective, and orally available inhibitor of human androgen receptor targeting its binding function-3 for the treatment of castration-resistant prostate cancer. *J Med Chem*. 2021;64:14968-14982.
79. Schröer J, Shenk T. Inhibition of cyclooxygenase activity blocks cell-to-cell spread of human cytomegalovirus. *Proc Natl Acad Sci U S A*. 2008;105:19468-19473.
80. Gramerc D, Peterlin Mašič L, Sollner Dolenc M. Bioactivation potential of thiophene-containing drugs. *Chem Res Toxicol*. 2014;27:1344-1358.
81. Baell J, Walters MA. Chemistry: chemical con artists foil drug discovery. *Nature*. 2014;513:481-483.
82. Glaser J, Holzgrabe U. Focus on PAINS: false friends in the quest for selective anti-protozoal lead structures from nature. *MedChemComm*. 2016;7:214-223.
83. Protti ÍF, Rodrigues DR, Fonseca SK, Alves RJ, Oliveira RB, Maltarollo VG. Do drug-likeness rules apply to oral prodrugs. *ChemMedChem*. 2021;16:1446-1456.
84. Lovering F, Bikker J, Humblet C. Escape from flatland: increasing saturation as an approach to improving clinical success. *J Med Chem*. 2009;52:6752-6756.
85. Lovering F. Escape from flatland 2: complexity and promiscuity. *MedChemComm*. 2013;4:515.
86. Jenster G, Van der Korput HAGM, Trapman J, Brinkmann AO. Identification of two transcription activation units in the n-terminal domain of the human androgen receptor. *J Biol Chem*. 1995;270:7341-7346.
87. McEwan IJ. Intrinsic disorder in the androgen receptor: identification, characterisation and drugability. *Mol BioSyst*. 2012;8:82-90.
88. Lavery DN, McEwan IJ. Structural characterization of the native NH₂-terminal transactivation domain of the human androgen receptor: a collapsed disordered conformation underlies structural plasticity and protein-induced folding. *Biochemistry*. 2008;47:3360-3369.
89. Lavery DN, McEwan IJ. Functional characterization of the native NH₂-terminal transactivation domain of the human androgen receptor: binding kinetics for interactions with TFIIF and SRC-1a. *Biochemistry*. 2008;47:3352-3359.
90. Yu X, Yi P, Hamilton RA, et al. Structural insights of transcriptionally active, full-length androgen receptor coactivator complexes. *Mol Cell*. 2020;79:812-823.e4.
91. Ruan H, Sun Q, Zhang W, Liu Y, Lai L. Targeting intrinsically disordered proteins at the edge of chaos. *Drug Discovery Today*. 2019;24:217-227.
92. Hay CW, McEwan IJ. The impact of point mutations in the human androgen receptor: classification of mutations on the basis of transcriptional activity. *PLoS One*. 2012;7:e32514.
93. Monaghan AE, Porter A, Hunter I, Morrison A, McElroy SP, McEwan IJ. Development of a high-throughput screening assay for small-molecule inhibitors of androgen receptor splice variants. *Assay Drug Dev Technol*. 2022;20:111-124.
94. Sadar MD. Small molecule inhibitors targeting the "achilles' heel" of androgen receptor activity. *Cancer Res*. 2011;71:1208-1213.
95. Lallous N, Dalal K, Cherkasov A, Rennie P. Targeting alternative sites on the androgen receptor to treat Castration-Resistant prostate cancer. *Int J Mol Sci*. 2013;14:12496-12519.
96. Hupe MC, Offermann A, Perabo F, et al. Inhibitoren des Androgenrezeptor-N-Terminus: zielgerichtete Therapien gegen die achillesferse verschiedener androgenrezeptormoleküle im fortgeschrittenen Prostatakarzinom. *Urologe*. 2018;57:148-154.
97. Sadar MD. Discovery of drugs that directly target the intrinsically disordered region of the androgen receptor. *Expert Opin Drug Discovery*. 2020;15:551-560.
98. Harvey A. Natural products in drug discovery. *Drug Discovery Today*. 2008;13:894-901.
99. David B, Wolfender JL, Dias DA. The pharmaceutical industry and natural products: historical status and new trends. *Phytochem Rev*. 2015;14:299-315.
100. Lahlou M. The success of natural products in drug discovery. *Pharmacol Pharm*. 2013;4:17-31.
101. NIC Staff. Discovering New Cancer Drugs from Nature. National Cancer Institute. 2019.
102. Choudhari AS, Mandave PC, Deshpande M, Ranjekar P, Prakash O. Phytochemicals in cancer treatment: from preclinical studies to clinical practice. *Front Pharmacol*. 2020;10:1614.
103. Sadar MD, Williams DE, Mawji NR, et al. Sintokamides A to E, chlorinated peptides from the sponge *Dysidea* sp. that inhibit transactivation of the N-terminus of the androgen receptor in prostate cancer cells. *Org Lett*. 2008;10:4947-4950.
104. Sadar MD, Mawji NR, Wang J, et al. Small molecule inhibitors of N-terminus activation of the androgen receptor. 2010.
105. Banuelos CA, Tavakoli I, Tien AH, et al. Sintokamide A is a novel antagonist of androgen receptor that uniquely binds activation function-1 in its amino-terminal domain. *J Biol Chem*. 2016;291:22231-22243.

106. Yan L, Banuelos CA, Mawji NR, Patrick BO, Sadar MD, Andersen RJ. Structure–activity relationships for the marine natural product sintokamides: androgen receptor N-terminus antagonists of interest for treatment of metastatic castration-resistant prostate cancer. *J Nat Prod*. 2021;84:797–813.
107. Meimetis LG, Williams DE, Mawji NR, et al. Niphatenones, glycerol ethers from the sponge *Niphates digitalis* block androgen receptor transcriptional activity in prostate cancer cells: structure elucidation, synthesis, and biological activity. *J Med Chem*. 2012;55:503–514.
108. Banuelos CA, Lal A, Tien AH, et al. Characterization of niphatenones that inhibit androgen receptor N-terminal domain. *PLoS One*. 2014;9:e107991.
109. Ramsewak RS, Nair MG, Strasburg GM, DeWitt DL, Nitiss JL. Biologically active carbazole alkaloids from *murrayakoenigii*. *J Agricult Food Chem*. 1999;47:444–447.
110. Nakahara K, Trakoontivakorn G, Alzoreky NS, Ono H, Onishi-Kameyama M, Yoshida M. Antimutagenicity of some edible Thai plants, and a bioactive carbazole alkaloid, mahanine, isolated from *micromelum minutum*. *J Agricult Food Chem*. 2002;50:4796–4802.
111. Amin KS, Jagadeesh S, Baishya G, et al. A naturally derived small molecule disrupts ligand-dependent and ligand-independent androgen receptor signaling in human prostate cancer cells. *Mol Cancer Ther*. 2014;13:341–352.
112. Yang Z, Luo H, Wang H, Hou H. Preparative isolation of bufalin and cinobufagin from Chinese traditional Medicine *ChanSu*. *J Chromatogr Sci*. 2008;46:81–85.
113. Hua Y, Azeem W, Shen Y, et al. Dual androgen receptor (AR) and STAT3 inhibition by a compound targeting the AR amino-terminal domain. *Pharmacol Res Perspect*. 2018;6:e00437.
114. Andersen RJ, Mawji NR, Wang J, et al. Regression of castrate-recurrent prostate cancer by a small-molecule inhibitor of the amino-terminus domain of the androgen receptor. *Cancer Cell*. 2010;17:535–546.
115. Myung JK, Banuelos CA, Fernandez JG, et al. An androgen receptor n-terminal domain antagonist for treating prostate cancer. *J Clin Invest*. 2013;123:2948–2960.
116. Brand LJ, Olson ME, Ravindranathan P, et al. EPI-001 is a selective peroxisome proliferator-activated receptor- γ modulator with inhibitory effects on androgen receptor expression and activity in prostate cancer. *Oncotarget*. 2015;6:3811–3824.
117. Yang YC, Banuelos CA, Mawji NR, et al. Targeting androgen receptor activation function-1 with EPI to overcome resistance mechanisms in castration-resistant prostate cancer. *Clin Cancer Res*. 2016;22:4466–4477.
118. De Mol E, Fenwick RB, Phang CTW, et al. EPI-001, a compound active against castration-resistant prostate cancer, targets transactivation unit 5 of the androgen receptor. *ACS Chem Biol*. 2016;11:2499–2505.
119. ESSA Pharmaceuticals. *Safety and Anti-Tumor Study of Oral EPI-506 for Patients With Metastatic Castration-Resistant Prostate Cancer [NCT02606123]*. 2015.
120. Banuelos CA, Ito Y, Obst JK, et al. Ralaniten sensitizes enzalutamide-resistant prostate cancer to ionizing radiation in prostate cancer cells that express androgen receptor splice variants. *Cancers*. 2020;12:1991.
121. Yin Y, Li R, Xu K, et al. Androgen receptor variants mediate DNA repair after prostate cancer irradiation. *Cancer Res*. 2017;77:4745–4754.
122. Martin SK, Banuelos CA, Sadar MD, Kyprianou N. N-terminal targeting of androgen receptor variant enhances response of castration resistant prostate cancer to taxane chemotherapy. *Mol Oncol*. 2015;9:628–639.
123. Kranzbühler B, Salemi S, Mortezaei A, Sulser T, Eberli D. Combined n-terminal androgen receptor and autophagy inhibition increases the antitumor effect in enzalutamide sensitive and enzalutamide resistant prostate cancer cells. *Prostate*. 2019;79:206–214.
124. Kato M, Banuelos CA, Imamura Y, et al. Cotargeting androgen receptor splice variants and mTOR signaling pathway for the treatment of castration-resistant prostate cancer. *Clin Cancer Res*. 2016;22:2744–2754.
125. Leung JK, Imamura Y, Kato M, Wang J, Mawji NR, Sadar MD. Pin1 inhibition improves the efficacy of ralaniten compounds that bind to the n-terminal domain of androgen receptor. *Commun Biol*. 2021;4:381.
126. Tien AH, Sadar MD. Cyclin-dependent kinase 4/6 inhibitor palbociclib in combination with ralaniten analogs for the treatment of androgen receptor-positive prostate and breast cancers. *Mol Cancer Ther*. 2022;21:294–309.
127. Le Moigne R, Banuelos CA, Mawji NR, et al. IND candidate EPI-7386 as an n-terminal domain androgen receptor inhibitor in development for the treatment of prostate cancer. *J Clin Oncol*. 2020;38:142.
128. Obst JK, Mawji NR, Teskey SJL, Wang J, Sadar MD. Differential gene expression profiles between N-terminal domain and ligand-binding domain inhibitors of androgen receptor reveal ralaniten induction of metallothionein by a mechanism dependent on MTF1. *Cancers*. 2022;14:386.
129. Hirayama Y, Tam T, Jian K, Andersen RJ, Sadar MD. Combination therapy with androgen receptor n-terminal domain antagonist EPI-7170 and enzalutamide yields synergistic activity in AR-V7-positive prostate cancer. *Mol Oncol*. 2020;14:2455–2470.
130. Nicolescu RCB, Maylin ZR, Pérez-Areales FJ, et al. Front cover: hybrid androgen receptor inhibitors outperform enzalutamide and EPI-001 in vitromodels of prostate cancer drug resistance. *ChemMedChem*. 2023;18:e202200548.

131. Sonehara K, Okada Y. Genomics-driven drug discovery based on disease-susceptibility genes. *Inflamm Regen*. 2021;41:8.
132. Entzeroth M, Flotow H, Condron P. Overview of high-throughput screening. *Curr Protoc Pharmacol*. 2009;44:1-27.
133. Johnston PA, Nguyen MM, Dar JA, et al. Development and implementation of a high-throughput high-content screening assay to identify inhibitors of androgen receptor nuclear localization in castration-resistant prostate cancer cells. *Assay Drug Dev Technol*. 2016;14:226-239.
134. Masoodi KZ, Eisermann K, Yang Z, et al. Inhibition of androgen receptor function and level in castration-resistant prostate cancer cells by 2-[(isoxazol-4-ylmethyl)thio]-1-(4-phenylpiperazin-1-yl)ethanone. *Endocrinology*. 2017;158:3152-3161.
135. Johnson JK, Skoda EM, Zhou J, et al. Small molecule antagonists of the nuclear androgen receptor for the treatment of castration-resistant prostate cancer. *ACS Med Chem Lett*. 2016;7:785-790.
136. Yang Z, Wang D, Johnson JK, et al. A novel small molecule targets androgen receptor and its splice variants in castration-resistant prostate cancer. *Mol Cancer Ther*. 2020;19:75-88.
137. Cole RN, Chen W, Pascal LE, Nelson JB, Wipf P, Wang Z. (+)-JJ-74-138 is a novel noncompetitive androgen receptor antagonist. *Mol Cancer Ther*. 2022;21:483-492.
138. Kim JG, Kang OY, Kim SM, et al. Synthesis and properties of pentafluorosulfanyl group (SF₅)-containing meta-diamide insecticides. *Molecules*. 2020;25:5536.
139. Rettig M, Jung ME, Elshan NGRD, An J. Inhibitors of the N-Terminal Domain of the Androgen Receptor. 2019.
140. Leeson PD, Young RJ. Molecular property design: does everyone get it. *ACS Med Chem Lett*. 2015;6:722-725.
141. Gupta M, Lee HJ, Barden CJ, Weaver DF. The blood-brain barrier (BBB) score. *J Med Chem*. 2019;62:9824-9836.
142. Ponnusamy S, Coss CC, Thiagarajan T, et al. Novel selective agents for the degradation of androgen receptor variants to treat castration-resistant prostate cancer. *Cancer Res*. 2017;77:6282-6298.
143. Ponnusamy S, He Y, Hwang DJ, et al. Orally bioavailable androgen receptor degrader, potential next-generation therapeutic for enzalutamide-resistant prostate cancer. *Clin Cancer Res*. 2019;25:6764-6780.
144. He Y, Hwang DJ, Ponnusamy S, et al. Exploration and biological evaluation of basic heteromonocyclic propanamide derivatives as SARs for the treatment of enzalutamide-resistant prostate cancer. *J Med Chem*. 2021;64:11045-11062.
145. Peng S, Wang J, Chen H, et al. Regression of castration-resistant prostate cancer by a novel compound QW07 targeting androgen receptor n-terminal domain. *Cell Biol Toxicol*. 2020;36:399-416.
146. Li H, Hassona MDH, Lack NA, et al. Characterization of a new class of androgen receptor antagonists with potential therapeutic application in advanced prostate cancer. *Mol Cancer Ther*. 2013;12:2425-2435.
147. Ban F, Leblanc E, Cavga AD, et al. Development of an androgen receptor inhibitor targeting the N-terminal domain of androgen receptor for treatment of castration resistant prostate cancer. *Cancers*. 2021;13:3488.
148. Goicochea NL, Garnovskaya M, Blanton MG, Chan G, Weisbart R, Lilly MB. Development of cell-penetrating bispecific antibodies targeting the n-terminal domain of androgen receptor for prostate cancer therapy. *Protein Eng Des Sel*. 2017;30:785-793.
149. Xie J, He H, Kong W, et al. Targeting androgen receptor phase separation to overcome antiandrogen resistance. *Nat Chem Biol*. 2022;18:1341-1350. doi:10.1038/s41589-022-01151-y
150. McEwan IJ. Breaking apart condensates. *Nat Chem Biol*. 2022;1292-1293.
151. Talele TT. Acetylene group, friend or foe in medicinal chemistry. *J Med Chem*. 2020;63:5625-5663.
152. Ban F, Dalal K, Li H, LeBlanc E, Rennie PS, Cherkasov A. Best practices of computer-aided drug discovery: lessons learned from the development of a preclinical candidate for prostate cancer with a new mechanism of action. *J Chem Inf Model*. 2017;57:1018-1028.
153. Shaffer PL, Jivan A, Dollins DE, Claessens F, Gewirth DT. Structural basis of androgen receptor binding to selective androgen response elements. *Proc Natl Acad Sci U S A*. 2004;101:4758-4763.
154. Narizhneva NV, Tararova ND, Ryabokon P, et al. Small molecule screening reveals a transcription-independent pro-survival function of androgen receptor in castration-resistant prostate cancer. *Cell Cycle*. 2009;8:4155-4167.
155. Zamagni A, Cortesi M, Zanoni M, Tesi A. Non-nuclear AR signaling in prostate cancer. *Front Chem*. 2019;7:651.
156. Veras Ribeiro Filho H, Tambones IL, Mariano Gonçalves Dias M, et al. Modulation of nuclear receptor function: targeting the protein-DNA interface. *Mol Cell Endocrinol*. 2019;484:1-14.
157. Li D, Zhou W, Pang J, et al. A magic drug target: androgen receptor. *Med Res Rev*. 2019;39:1485-1514.
158. Nickols NG, Dervan PB. Suppression of androgen receptor-mediated gene expression by a sequence-specific DNA-binding polyamide. *Proc Natl Acad Sci U S A*. 2007;104:10418-10423.
159. Yang F, Nickols NG, Li BC, Marinov GK, Said JW, Dervan PB. Antitumor activity of a pyrrole-imidazole polyamide. *Proc Natl Acad Sci U S A*. 2013;110:1863-1868.
160. Hargrove AE, Martinez TF, Hare AA, et al. Tumor repression of VCaP xenografts by a pyrrole-imidazole polyamide. *PLoS One*. 2015;10:e0143161.

161. Chenoweth DM, Harki DA, Dervan PB. Solution-phase synthesis of pyrrole-imidazole polyamides. *J Am Chem Soc.* 2009;131:7175-7181.
162. Kurmis AA, Yang F, Welch TR, Nickols NG, Dervan PB. A pyrrole-imidazole polyamide is active against enzalutamide-resistant prostate cancer. *Cancer Res.* 2017;77:2207-2212.
163. Yang F, Nickols NG, Li BC, et al. Animal toxicity of hairpin pyrrole-imidazole polyamides varies with the turn unit. *J Med Chem.* 2013;56:7449-7457.
164. Kurmis AA, Dervan PB. Sequence specific suppression of androgen receptor-DNA binding in vivo by a Py-Im polyamide. *Nucleic Acids Res.* 2019;47:3828-3835.
165. Jones JO, Diamond MI. A cellular conformation-based screen for androgen receptor inhibitors. *ACS Chem Biol.* 2008;3:412-418.
166. Jones JO, Bolton EC, Huang Y, et al. Non-competitive androgen receptor inhibition in vitro and in vivo. *Proc Natl Acad Sci U S A.* 2009;106:7233-7238.
167. Li H, Ban F, Dalal K, et al. Discovery of small-molecule inhibitors selectively targeting the DNA-binding domain of the human androgen receptor. *J Med Chem.* 2014;57:6458-6467.
168. Dalal K, Roshan-Moniri M, Sharma A, et al. Selectively targeting the DNA-binding domain of the androgen receptor as a prospective therapy for prostate cancer. *J Biol Chem.* 2014;289:26417-26429.
169. Pal SK, Tew BY, Lim M, et al. Mechanistic investigation of the androgen receptor DNA-binding domain inhibitor pyrvinium. *ACS Omega.* 2019;4:2472-2481.
170. Lim M, Otto-Duessel M, He M, et al. Ligand-independent and tissue-selective androgen receptor inhibition by pyrvinium. *ACS Chem Biol.* 2014;9:692-702.
171. Momtazi-Borojeni AA, Abdollahi E, Ghasemi F, Caraglia M, Sahebkar A. The novel role of pyrvinium in cancer therapy. *J Cell Physiol.* 2018;233:2871-2881.
172. Brodie J, McEwan IJ. Intra-domain communication between the n-terminal and DNA-binding domains of the androgen receptor: modulation of androgen response element DNA binding. *J Mol Endocrinol.* 2005;34:603-615.
173. Borgmann H, Dalal K, Beraldi E, Cherkasov A, Rennie P, Gleave M. 40 Efficacy of prostate cancer compound with novel mechanism of action targeting the DNA binding domain of the androgen receptor. *Eur Urol Suppl.* 2016;15:e40.
174. Dalal K, Che M, Que NS, et al. Bypassing drug resistance mechanisms of prostate cancer with small molecules that target androgen Receptor-Chromatin interactions. *Mol Cancer Ther.* 2017;16:2281-2291.
175. Tcherkassov A, Rennie PS, Ban F, Li H, Joseph E, Leblanc J. Human androgen receptor Dna-binding domain (Dbd) compounds as therapeutics and methods for their use. 2015.
176. Xu R, Tian Y, Huang S, et al. Synthesis and evaluation of novel thiazole-based derivatives as selective inhibitors of DNA-binding domain of the androgen receptor. *Chem Biol Drug Des.* 2018;91:172-180.
177. Dalal K, Ban F, Li H, et al. Selectively targeting the dimerization interface of human androgen receptor with small-molecules to treat castration-resistant prostate cancer. *Cancer Lett.* 2018;437:35-43.
178. van Royen ME, van Cappellen WA, de Vos C, Houtsmuller AB, Trapman J. Stepwise androgen receptor dimerization. *J Cell Sci.* 2012;125:1970-1979.
179. Mizutani T, Suzuki K. Relative hepatotoxicity of 2-(substituted phenyl)thiazoles and substituted thiobenzamides in mice: evidence for the involvement of thiobenzamides as ring cleavage metabolites in the hepatotoxicity of 2-phenylthiazoles. *Toxicol Lett.* 1996;85:101-105.
180. Radaeva M, Ban F, Zhang F, et al. Development of novel inhibitors targeting the D-box of the DNA binding domain of androgen receptor. *Int J Mol Sci.* 2021;22:2493.
181. Rademacher PM, Woods CM, Huang Q, Szklarz GD, Nelson SD. Differential oxidation of two thiophene-containing regioisomers to reactive metabolites by cytochrome P450 2C9. *Chem Res Toxicol.* 2012;25:895-903.
182. Kafka M, Mayr F, Temml V, et al. Dual inhibitory action of a novel AKR1C3 inhibitor on both full-length AR and the variant AR-V7 in enzalutamide resistant metastatic castration resistant prostate cancer. *Cancers.* 2020;12:2092.
183. Steckelbroeck S, Jin Y, Gopishetty S, Oyesanmi B, Penning TM. Human cytosolic 3 α -hydroxysteroid dehydrogenases of the aldo-keto reductase superfamily display significant 3 β -hydroxysteroid dehydrogenase activity. *J Biol Chem.* 2004;279:10784-10795.
184. Lee GT, Nagaya N, Desantis J, et al. Effects of MTX-23, a novel PROTAC of androgen receptor splice variant-7 and androgen receptor, on CRPC resistant to second-line antiandrogen therapy. *Mol Cancer Ther.* 2021;20:490-499.
185. Pike A, Williamson B, Harlfinger S, Martin S, McGinnity DF. Optimising proteolysis-targeting chimeras (PROTACs) for oral drug delivery: a drug metabolism and pharmacokinetics perspective. *Drug Discovery Today.* 2020;25:1793-1800.
186. Congreve M, Carr R, Murray C, Jhoti H. A 'rule of three' for fragment-based lead discovery. *Drug Discovery Today.* 2003;8:876-877.

187. Zhou ZX, Sar M, Simental JA, Lane MV, Wilson EM. A ligand-dependent bipartite nuclear targeting signal in the human androgen receptor. requirement for the DNA-binding domain and modulation by NH2-terminal and carboxyl-terminal sequences. *J Biol Chem.* 1994;269:13115-13123.
188. Wang Q, Lu J, Yong EL. Ligand- and coactivator-mediated transactivation function (AF2) of the androgen receptor ligand-binding domain is inhibited by the cognate hinge region. *J Biol Chem.* 2001;276:7493-7499.
189. Tanner T, Claessens F, Haelens A. The hinge region of the androgen receptor plays a role in Proteasome-Mediated transcriptional activation. *Ann NY Acad Sci.* 2004;1030:587-592.
190. Céraline J, Cruchant MD, Erdmann E, et al. Constitutive activation of the androgen receptor by a point mutation in the hinge region: a new mechanism for androgen-independent growth in prostate cancer: constitutive activation of the androgen receptor. *Int J Cancer.* 2004;108:152-157.
191. Haelens A, Tanner T, Denayer S, Callewaert L, Claessens F. The hinge region regulates DNA binding, nuclear translocation, and transactivation of the androgen receptor. *Cancer Res.* 2007;67:4514-4523.
192. Tanner TM, Denayer S, Geverts B, et al. A 629RKLKK633 motif in the hinge region controls the androgen receptor at multiple levels. *Cell Mol Life Sci.* 2010;67:1919-1927.
193. Deeb A, Jääskeläinen J, Dattani M, Whitaker HC, Costigan C, Hughes IA. A novel mutation in the human androgen receptor suggests a regulatory role for the hinge region in amino-terminal and carboxy-terminal interactions. *J Clin Endocrinol Metab.* 2008;93:3691-3696.
194. Clinckemalie L, Vanderschueren D, Boonen S, Claessens F. The hinge region in androgen receptor control. *Mol Cell Endocrinol.* 2012;358:1-8.
195. Bianchini D, Omlin A, Pezaro C, et al. First-in-human phase I study of EZN-4176, a locked nucleic acid antisense oligonucleotide to exon 4 of the androgen receptor mRNA in patients with castration-resistant prostate cancer. *Br J Cancer.* 2013;109:2579-2586.
196. Zhang Y, Castaneda S, Dumble M, et al. Reduced expression of the androgen receptor by third generation of antisense shows antitumor activity in models of prostate cancer. *Mol Cancer Ther.* 2011;10:2309-2319.
197. Lee YH, Kwak J, Choi HK, et al. EGCG suppresses prostate cancer cell growth modulating acetylation of androgen receptor by anti-histone acetyltransferase activity. *Int J Mol Med.* 2012;30:69-74.
198. Yamashita S, Lai KP, Chuang KL, et al. ASC-J9 suppresses castration-resistant prostate cancer growth through degradation of full-length and splice variant androgen receptors. *Neoplasia.* 2012;14:74-83.
199. Cheng MA, Chou FJ, Wang K, et al. Androgen receptor (AR) degradation enhancer ASC-J9® in an FDA-approved formulated solution suppresses castration resistant prostate cancer cell growth. *Cancer Lett.* 2018;417:182-191.
200. Loddick SA, Ross SJ, Thomason AG, et al. AZD3514: a small molecule that modulates androgen receptor signaling and function in vitro and in vivo. *Mol Cancer Ther.* 2013;12:1715-1727.
201. Mak KK, Epemolu O, Pichika MR. The role of DMPK science in improving pharmaceutical research and development efficiency. *Drug Discovery Today.* 2022;27:705-729.
202. Waltering KK, Urbanucci A, Visakorpi T. Androgen receptor (AR) aberrations in castration-resistant prostate cancer. *Mol Cell Endocrinol.* 2012;360:38-43.
203. Azad AA, Volik SV, Wyatt AW, et al. Androgen receptor gene aberrations in circulating cell-free DNA: biomarkers of therapeutic resistance in castration-resistant prostate cancer. *Clin Cancer Res.* 2015;21:2315-2324.

AUTHOR BIOGRAPHIES

Christopher M. Riley was awarded a PhD in Medicinal Chemistry in 2021, supervised by Dr. Craig Jamieson at the University of Strathclyde. The focus of this research was small molecule inhibition of the Androgen Receptor for the treatment of advanced Prostate Cancer. Following the completion of his PhD studies, Dr. Riley has been involved in the development of isoform-selective kinase inhibitors and DNA-binding polyamide therapeutics in the research groups of Professors Simon Mackay and Glenn Burley, respectively.

Jessica M. L. Elwood received her MChem degree in 2016 from Bangor University. She obtained her PhD in Total Synthesis in 2021 from the University of Glasgow under the supervision of Professor J. S. Clark. Jessica then went on to carry out Postdoctoral Research at the University of Strathclyde in collaboration with the University of Aberdeen where her research focused on synthesizing and developing novel small molecules for the treatment of Castrate Resistant Prostate Cancer.

Martyn C. Henry earned a first-class MChem degree from Heriot-Watt University in 2016 and a PhD from the University of Glasgow in 2020. Martyn is now a postdoctoral research associate in the Jamieson Group at the University of Strathclyde. His research focuses on the design and synthesis of small-molecule inhibitors of the androgen receptor for the treatment of castration-resistant prostate cancer.

Irene Hunter is a Research Fellow with extensive experience in the areas of biochemistry, cell biology, and cell signaling. She works on androgen receptor signaling in prostate cancer and novel mechanisms of inhibiting receptor activity.

J. Daniel Lopez-Fernandez graduated with a first-class MSc degree from the University of Santiago de Compostela in 2010. Following a spell in industry, Daniel then earned his PhD from Newcastle University under the supervision of Ian R. Hardcastle and Michael J. Waring, in the area of medicinal chemistry. In 2020, Daniel worked as a Postdoctoral Research Associate in the Jamieson Group. His research was focused on the design and synthesis of small molecule inhibitors of the androgen receptor.

Iain J. McEwan obtained his PhD from the University of Glasgow. He is a Professor of Molecular Endocrinology at the University of Aberdeen and his research focuses on fundamental and translational aspects of steroid receptor structure and function in health and disease.

Craig Jamieson earned his PhD in Biological Chemistry at the University of Edinburgh in 1999. After post-doctoral work in Cambridge, he joined the pharmaceutical industry (GSK, Merck) in 2001 before moving to The University of Strathclyde in 2010. His interests are in the general area of chemical biology and medicine discovery, where he collaborates with Iain McEwan in the area of prostate cancer research.

How to cite this article: Riley CM, Elwood JML, Henry MC, et al. Current and emerging approaches to noncompetitive AR inhibition. *Med Res Rev.* 2023;43:1701-1747. doi:10.1002/med.21961